

**The Unfolded Protein Response in Fission Yeast:
Ire1 Modulates Stability of Select mRNAs to
Maintain Protein Homeostasis**

Von der Fakultät Energie-, Verfahrens- und Biotechnik der Universität Stuttgart
zur Erlangung der Würde eines Doktors der Naturwissenschaften (Dr. rer. nat.)
genehmigte Abhandlung

Vorgelegt von

Dipl.-Biol (t.o.)

Philipp Kimmig

geboren in Engen/Hegau

Hauptberichter: Prof. Dr. Dieter H. Wolf

Mitberichter: Priv. Doz. Dr. Hans Rudolph

Tag der Mündlichen Prüfung: 4. März 2013

Institut für Biochemie der Universität Stuttgart

2013

Eidesstattliche Erklärung

Hiermit versichere ich, dass ich diese Arbeit selbst verfasst und dabei keine anderen als die angegebenen Quellen und Hilfsmittel verwendet habe.

Absberg, November 2012

Philipp Kimmig

Table of Contents

Abbreviations	7
Abstract	9
Zusammenfassung	11
1. Introduction	13
1.1 From Gene Expression to Protein Synthesis	13
1.2 Protein Folding and Degradation	14
1.3 The Secretory Pathway	14
1.4 The Endoplasmic Reticulum (ER)	15
1.5 Protein Folding, Modifications and Quality Control in the ER	16
1.6 The Unfolded Protein Response	17
1.6.1 Historical Aspects of the Unfolded Protein Response	17
1.6.2 The Ire1-Hac1/XBP1 Branch in Yeast and Metazoans	18
1.6.3 PERK and ATF6, Two Additional UPR Branches in Metazoans	21
1.6.4 Post-transcriptional Output of the UPR	23
2. Results	25
2.1 Ire1 Down-Regulates Select mRNAs upon ER Stress	25
2.1.1 The Ire1-Hac1 Branch is not Conserved in Fission Yeast	25
2.1.2 Ire1 is Essential to Cope with ER Stress	26
2.1.3 ER Stress-dependent mRNA Down-Regulation	27
2.1.5 Ire1 Down-Regulates mRNAs Encoding Ergosterol Biosynthesis Proteins	31
2.1.6 Ire1 Cleaves Down-Regulated mRNAs at Specific Sites	32
2.1.7 Importance of the 3'->5' mRNA Degradation Machinery to Cope with ER Stress	34
2.1.8 Genome-Wide Identification of Specific Ire1 Cleavage Sites	35
2.1.9 ORF of <i>Gas2</i> mRNA is Sufficient to Down-Regulate mRNA	37
2.1.10 Mutational Analysis of Ire1 Cleavage Site in <i>Gas2</i> mRNA Reporter	38
2.2. <i>Bip1</i> mRNA Processing in Response to ER stress	39
2.2.1 <i>Bip1</i> mRNA Changes Sizes and Increases upon ER Stress	39
2.2.3 <i>Bip1</i> mRNA is Truncated in its 3' UTR upon ER Stress	42
2.2.4 3' UTR of <i>Bip1</i> mRNA and Signal Sequence are Sufficient to Induce Truncation	44
2.2.5 Mutational Analysis of <i>Bip1</i> mRNA Cleavage Site	45
2.2.6 <i>Bip1</i> mRNA Processing Represents a Singularity	46
2.2.7 Truncated <i>Bip1</i> mRNA is Efficiently Translated	46
2.2.8 <i>Bip1</i> mRNA Processing is Important for Cell Fitness	48
3. Discussion	51
The Unfolded Protein Response in Fission Yeast	51
The Physiological Role of RIDD in <i>S. pombe</i>	51
RNA Cleavage and Recognition	53
Processing of <i>Bip1</i> mRNA	54
Conclusion	57
4. Materials and Methods	59
4.1 Nomenclature	59
4.2 Molecular Biology methods	59
4.3 Microbiological methods	63

4.4	Genome-wide methods	65
4.5	Protein biochemistry	68
5.	Bibliography	70
6.	Acknowledgment	76
7.	Curriculum vitae	77

Abbreviations

ATP	Adenosine 5'-triphosphate
bZIP	Basic leucine zipper domain
DNA	Desoxyribonucleic acid
DTT	Dithiothreitol
<i>E. coli</i>	<i>Escherichia coli</i>
ER	Endoplasmic reticulum
ERAD	ER-associated degradation
Fig	Figure
g	Grams
GFP	Green fluorescent protein
Hsp	Heat shock protein
kDa	Kilodalton
l	Litre
mRNA	Messenger RNA
PDI	Protein disulfide isomerase
Poly(A)	Polyadenylation
RNA	Ribonucleic acid
rRNA	Ribosomal Ribonucleic acid
<i>S. cerevisiae</i>	<i>Saccharomyces cerevisiae</i>
<i>S. pombe</i>	<i>Schizosacharomyces pombe</i>
Tm	Tunicamycin
tRNA	Transfer RNA

UPR	Unfolded protein response
UPS	Ubiquitin-proteasome-system
UTR	Untranslated region
WT	Wild type

Abstract

Virtually all proteins that eukaryotic cells display on their surface or that are secreted into the extracellular space are first folded and assembled in the membrane-surrounded organelle endoplasmic reticulum (ER). Only properly folded and assembled proteins depart from the ER to the cell surface. If the ER does not have enough capacity to fold, a condition termed “ER stress”, a signal pathway called the “Unfolded Protein Response” (UPR), is switched on to increase the protein folding capacity, to expand the surface area and volume of the compartment.

All eukaryotic cells, from unicellular yeasts to mammalian cells, contain a highly conserved protein-folding sensor Ire1. In all species analyzed to date, Ire1, an ER membrane-resident kinase/endoribonuclease, is known to activate the UPR through an unconventional messenger RNA (mRNA) splicing mechanism to induce translation of a potent transcription factor Hac1 (in yeast) or XBP1 (in metazoans). This unique splicing event provides the switch that drives a comprehensive gene expression program in which the production of ER components is increased to boost the protein folding capacity of the compartment.

In this thesis an organism is identified, the yeast *Schizosaccharomyces pombe*, in which the UPR does not involve mRNA splicing or the initiation of a gene expression program to increase the folding capacity of the ER. Rather *Schizosaccharomyces pombe* lacking, a Hac1/XBP1 ortholog, utilizes Ire1 RNase activity to an entirely different end. We found that activation of Ire1 in *S. pombe* leads to the decay of a specific class of mRNAs that all encode proteins entering the ER. Interestingly, the set of down-regulated mRNA targets are particularly enriched for those encoding proteins involved in sterol metabolism, suggesting a potential qualitative change of the physiology of the cell.

The deletion of the cytosolic mRNA degradation pathway shows an accumulation of RNA cleavage fragments of the down-regulated mRNA targets upon ER stress, an event by means that the Ire1 endonuclease directly cleaves these mRNAs. Intriguingly, the down-regulated mRNAs contain a short three-nucleotide base UG/C consensus at the Ire1 cut sites where cleavage occurs after G.

Thus, rather than increasing the protein folding capacity of the ER when faced with an increased protein folding load, *S. pombe* cells correct the imbalance by decreasing the load via mRNA cleavage.

Besides decreasing the ER load, a single mRNA—the mRNA that encodes the molecular chaperone BiP, which is one of the major protein-folding components in the ER—uniquely escapes this decay. Rather than being degraded, Ire1 truncates *Bip1* mRNA in its 3' UTR, which—counter-intuitively stabilizes the non-polyadenylated 5' fragment and results in increased Bip1 translation.

Decreasing the protein load by selective mRNA degradation and the single up-regulation of the major chaperone in the ER illustrate how a universally conserved machinery has been invented to maintain ER homeostasis in fission yeast.

Zusammenfassung

Der Großteil aller sekretorischen Proteine in eukaryotischen Zellen, entweder Plasmamembran Proteine oder Proteine die in den extrazellulären Raum sekretiert werden, durchlaufen das membranumschlossene Endoplasmatische Retikulum (ER), wo sie gefaltet und zu Komplexen zusammengesetzt werden. Nur korrekt gefaltete und zusammengesetzte Proteine im ER werden bis zur Zelloberfläche weitergeleitet. Falls das ER nicht über ausreichende Kapazitäten zur Proteinfaltung verfügt, ein Zustand den man auch „ER Stress“ bezeichnet, wird daraufhin ein Signalweg angeschaltet, der sogenannte “Unfolded Protein Response” (UPR), der eine Erhöhung der Proteinfaltungskapazität im ER zur Folge hat und das Volumen des Kompartiments erweitert.

Alle eukaryotischen Zellen, von Einzellern wie Hefe bis zu menschlichen Zellen, besitzen einen hochkonservierten Proteinfaltungs-Sensor Ire1, eine ER-Transmembran-Protein-Kinase/Endoribonuklease. In allen bisher analysierten Spezies initiiert Ire1 den “Unfolded Protein Response” mittels einer unkonventionellen mRNA Spleißreaktion, was zur Translation und Aktivierung eines potenten Transkriptionsfaktor Hac1 (in Hefe) oder XBP1 (in Metazoen) führt. Diese einzigartige Spleißreaktion fungiert als eine Art Schalter, welcher bei Aktivierung ein umfangreiches Expressionsprogramm auslöst, um die Proteinfaltungsmaschinerie zu erweitern und das Volumen des Kompartiment zu vergrößern.

In dieser Arbeit konnte erstmals gezeigt werden, dass der UPR einen Mechanismus auslösen kann, der weder eine mRNA Spleißreaktion, noch ein Transkriptionsprogramm für die Erhöhung der Kapazität der Proteinfaltung im ER induziert. Vielmehr benutzt die Hefe *Schizosaccharomyces pombe*, die keinerlei Hac1/XBP1 Orthologe besitzt, Ire1 auf eine komplett andere Art und Weise. Die Aktivierung von Ire1 in *S. pombe* führt zu einem Abbau von selektionierten mRNAs, die alle für sekretorische Proteine kodieren. Dabei ist festzustellen, dass eine signifikante Anzahl der abgebauten mRNAs, für Proteine kodieren, die im Sterol-Metabolismus involviert sind, was auf eine mögliche qualitative Veränderung der Zellphysiologie hinweisen könnte.

Durch das Ausschalten des zytosolischen Abbauweges für mRNAs konnten endonukleolytische mRNA Zwischensprodukte stabilisiert werden, was darauf hinweist, dass Ire1 diese mRNAs direkt schneidet. Interessanterweise teilen diese abgebauten mRNAs eine

Konsensus-Sequenz in ihrer von Ire1 geschnittenen Sequenz, die aus den drei Basenpaaren UG/C bestehend, wobei Ire1 nach dem Nukleotid G schneidet.

Im Gegensatz zu einer Vergrößerung der Faltungsmaschinerie bei erhöhter Konzentration an fehlgefalteten Protein im ER, korrigiert *S. pombe* also das Ungleichgewicht letztendlich durch Verringerung des Proteinimportes bei gleichbleibender Kapazität der Proteinfaltung.

Neben der Drosselung des Proteinimports in das ER, entgeht eine einzelne mRNA, die von BiP, eines der wichtigsten Faltungshelfer im ER, diesem Abbaumechanismus. Statt einer Degradation wird die *Bip1* mRNA innerhalb der 3' UTR durch Ire1 geschnitten und verkürzt, was entgegen den Erwartungen, das nicht-polyadenylierte 5' Fragment stabilisiert und die Translation von Bip1 erhöht.

Die Reduktion des Proteinimports in das ER durch den selektiven Abbau von mRNAs und die Erhöhung eines einzelnen Chaperons im ER veranschaulicht, wie eine omnipräsente konservierte Maschinerie für die Erhaltung des ER Gleichgewichts variiert wurde.

1. Introduction

The universal building block of all life on earth is a cell. Organisms exist as single cells or as aggregates forming a multicellular organism, such as humans, contain more than 10 trillion cells. Every single cell carries the heredity (genetic) information, defining its own construction plan and capable of generating a new cell, completed with a new copy of the genetic information. Therefore an individual cell is the minimal self-reproducing unit.

In principle, there are two main categories of cells: prokaryotes and eukaryotes. Traditionally prokaryotes were classified in one group, but it now appears that they are divided into two distinct groups, bacteria and archaea [1].

In general eukaryotic cells are bigger and more elaborate than prokaryotes. This increase in complexity of eukaryotic cells is accompanied by the existence of an intricate system of intracellular compartments unlike bacteria, which generally consist of a single intracellular compartment. These different membrane-enclosed compartments, or organelles, within a eukaryotic cell allow diverse functions and regulations under specific chemical environments. Hereby each organelle contains its own characteristic set of enzymes, a unique lipid composition of its membrane and specific transport systems to accomplish the flow of molecules and information from one compartment to another. One of these internal compartments, the nucleus, is by definition the locus where the genetic information is stored in form of a linear biopolymer called deoxyribonucleic acid (DNA). Besides its role for storing the genetic information for cell replication, the same segment of DNA can be used for synthesis of two other key classes of polymers, RNA and proteins, whereby RNA functions as a precursor molecule to synthesize proteins. As enzymes, proteins are catalyzing most chemical reactions in all living cells, but also accomplishing other functions, as maintaining structures, generating movement and sensing signals. The flow of genetic information from DNA to messenger RNA (mRNA) to protein is the central dogma of Molecular Biology [1].

1.1 From Gene Expression to Protein Synthesis

At the beginning of mRNA synthesis, certain sections of the double-stranded DNA are transcribed into pre-mRNAs, catalyzed by the RNA polymerase II, which uses one strand of the DNA double helix as a template. Immediately following its synthesis, pre-mRNA undergoes several processing steps, including splicing to remove non-coding sequences

(introns), incorporation of a 5' 7 methylguanosine cap structure at the 5' end and adding a 3' poly(A) tail by the poly(A) polymerase to the mRNA. These two modifications are playing a crucial role in mRNA stability and in the translation of proteins. After several quality control steps the mature mRNA is transported through the nuclear pore complex into the cytosol, the site of protein synthesis. Besides the transcription of mRNA molecules coding for proteins, two other important RNA species are transcribed: transfer RNA (tRNA) and ribosomal RNA (rRNA). In the cytosol a ribonucleoprotein complex called ribosome binds to the start site of mRNAs near the 5' UTR and initiates translation of the coding sequence [1].

1.2 Protein Folding and Degradation

Immediately after translation, proteins start to fold into their correct conformation. To avoid protein aggregations molecular chaperons recognize exposed hydrophobic patches of unfolded proteins and assist to fold them into their proper conformation by using energy from ATP hydrolysis [2]. The major group of chaperons belongs to the heat-shock family. When cells are exposed to high temperature (heat-shock), this class of enzymes is dramatically synthesized to counteract the heat induced folding stress. If proteins fail to fold correctly in a certain time, they become substrates for the protein degradation machineries. The most prominent degradation pathway is the ubiquitin-proteasome-system (UPS) [3]. Ubiquitin is covalently added to a misfolded protein by an ubiquitin ligase, resulting in a polyubiquitin chain and becoming a substrate of the proteasome. The proteasome thereby moves the entire protein into its interior where protease activities hydrolyze the protein. This pathway plays a significant role in maintaining protein homeostasis in all eukaryotic cells. Imbalance of the protein homeostasis can have dramatic outcomes for cells. In fact there are various diseases that derive from this imbalance, for instance Alzheimer- and Parkinson-disease [4,5].

1.3 The Secretory Pathway

To communicate with it's outside and quickly respond to changing environments, cells adjust the composition of their plasma membrane or secrete molecules according to need. The main biosynthetic pathway for delivering new proteins and lipids to the plasma membrane or to release molecules into the extracellular space is the secretory pathway [1]. The journey of these proteins has its origins in the endoplasmic reticulum (ER), the most abundant organelle

in the cell. The proteins transit then from the ER through the Golgi apparatus, finally ending up in vesicles that are transiently fused at the plasma membrane. At each step along the way there are crucial quality steps and modifications that determine how and if the protein will proceed. This quality control system plays a crucial role for all eukaryotic cells. For instance exposing wrongly folded proteins at the surface can have drastic consequences for cells and for the entire organism. Approximately one third of all proteins are traversing through the secretory pathway, the endoplasmic reticulum serves as the first way station.

1.4 The Endoplasmic Reticulum (ER)

The endoplasmic reticulum consists of a network labyrinth of membrane tubules and sheets within all eukaryotic cells. The ER lumen provides an environment which is extracytosolic and therefore topologically equivalent to the extracellular space. It is composed of a monolayer of membranes, which makes it a highly dynamic compartment [6,7]. The ER plays a central role in lipid biosynthesis, calcium storage, and facilitates protein folding. These various functions of the ER are essential for every eukaryotic cell, but can vary greatly between different cell types and different conditions. To accommodate different demands cells subdivide the ER into two different types: rough ER (rER), because of attached ribosome, and smooth ER (sER), ribosome-free in a tubular structure [1,8]

In all eukaryotes there are two major pathways by which proteins are transported across the ER membrane or integrated as transmembrane proteins. In the post-translation pathway, polypeptides are completed in the cytosol before entering the ER compartment. In the co-translational pathway transport occurs while the polypeptide is synthesized on a ribosome and the membrane-bound ribosome translocates the polypeptide through a translocon [9]. This protein transport by the translating ribosomes to the translocon is facilitated by the signal recognition complex (SRP) [10-12]. Structurally, the SRP can be defined as a ribonucleoprotein complex, consisting of six different polypeptides and one RNA molecule. In the cytosol, when the signal sequence emerges from the ribosome exit tunnel at the beginning of protein synthesis, SRP identifies a short signal sequence defined as a sequence of 5-35 amino acids at the N-terminus of the protein containing a hydrophobic stretch [13]. Through a tight binding to the signal sequence, SRP induces a translational arrest of the ribosome and transfers it to the ER membrane through binding of the signal recognition receptor. Both steps use the energy of GTP hydrolysis [14,15]. After targeting, polypeptides

are transported through the ER membrane at specific translocation sites, called the Sec61 translocon [16-18]. Immediately after entering the lumen of the ER chaperones are assisting to fold the unfolded polypeptide.

1.5 Protein Folding, Modifications and Quality Control in the ER

When proteins enter as nascent polypeptides the ER lumen, the signal sequence is rapidly cleaved off by the signal peptidase [19]. Because of its folding state a nascent polypeptide is immediately recognized by molecular chaperones to assist the folding process. One of this ER-resident chaperones is the Hsp70 BiP (in *S. cerevisiae* Kar2; in *S. pombe* Bip1), one of the most abundant proteins in the ER [2,20]. Besides its universal role in protein folding, BiP facilitates the process of protein translocation through the translocon into the ER by pulling proteins [21].

One of the important posttranslational modifications is the formation of disulfide bonds (S-S) within a protein. In general disulfide bonds stabilize protein conformations, which are particularly important for secreted proteins. The ER-resident protein PDI (protein disulfide isomerase) catalyzes the oxidation of free sulfhydryl (SH) groups on cysteines to form proper disulfide bonds [22].

Another common modification is the covalent addition of sugars to proteins in the ER. This process involves the transfer of an oligosaccharide precursor en bloc to a specific amino acid sequence Asn-X-Ser or Asn-X-Thr (where X is any amino acid except proline). The sugar is thereby covalently linked by to the side-chain of asparagine (N-linked glycosylation) [23]. Immediately upon addition of the sugar, two glucoses are removed by glucosidase I and II. This monoglucosylated glycosylated protein can interact with calnexin and calreticulin, both functioning as chaperones and lectins. Cleavage of the remaining glucose by glucosidase II terminates the interaction with both chaperones/lectins. If the protein is still incompletely folded it is scanned by UGGT (UDP-glucose:glycoprotein glucosyltransferase), which re-glucosylates the protein and initiates another round of the cycle. The cycle of glucosylation and de-glucosylation continues until the protein achieves its fully folded state or is target for degradation [24,25].

Despite having a sophisticated folding machinery, many translocated proteins fail to achieve their properly folded state in the ER. To avoid accumulation of misfolded proteins, cells employ a unique degradation process, called ER-associated degradation (ERAD), to cope with this problem [26-28]. The ERAD system eliminates misfolded proteins via degradation in the cytosol. Therefore, misfolded proteins are retrotranslocated across the ER membrane into the cytosol, where ubiquitin conjugating enzymes together with ubiquitin ligases target them for proteasomal degradation [26,27].

To identify misfolded proteins, cells use the N-glycosylation state of the protein. Cleaving off two extra mannose molecules initiates the degradation of misfolded proteins. Yos9 (in yeast) [29], another lectin protein, binds and transfers the marked misfolded protein to ER transmembrane ubiquitin ligases [27]. Thereupon the substrate is pushed through the retrotranslocon into the cytosol where it is ubiquitinated and degraded by the proteasome [27].

Another important process to cope with accumulation of misfolded proteins in the ER is the unfolded protein response (UPR), which transmits a signal from the ER to the nucleus to up-regulate chaperones and lipid synthesis [30]. Intriguingly another major output of the UPR is the up-regulation of the ERAD machinery, suggesting coordination between the two systems. In fact, a double deletion of an ERAD- and an UPR-component causes synthetic lethality in yeast, highlighting this model [31,32].

1.6 The Unfolded Protein Response

Environmental or physiological demands can lead to an imbalance between the protein folding load and the protein folding capacity in the ER lumen, resulting in an accumulation of unfolded or misfolded proteins, a condition termed “ER stress”. The unfolded protein response operates in all eukaryotic cells to adjust the protein folding capacity and lipid synthesis of the endoplasmic reticulum according to need. Examples include activation of the UPR during meiosis and cell differentiation [33]. Besides its cytoprotective function, when unmitigated ER stress is toxic to cells and triggers cell death [30,34-36].

1.6.1 Historical Aspects of the Unfolded Protein Response

The signaling components of the UPR were first discovered in *Saccharomyces cerevisiae*. Mori and coworkers identified a 22bp DNA sequence, known as the unfolded protein

response element (UPRE), in the promoter of BiP (in *S. cerevisiae* Kar2), which is activated in response to accumulation of unfolded protein in the ER [37]. This short element was sufficient for transcriptional activation of a heterologous promoter driving a reporter gene upon ER stress. By using this transcriptional reporter, the Mori lab and the Walter lab simultaneously identified mutants by a genetic screen, blocking activation of the UPR-inducible reporter. In both studies, they identified the gene Ire1 (inositol requiring enzyme 1), coding for an ER-resident transmembrane kinase/endoribonuclease [38,39]. Ire1 is sensing and transmitting the signal from the ER into the cytosol. Later, the Walter lab identified a second component of the pathway coding for the missing bZIP transcription factor Hac1 (in metazoans XBP1) [40]. In the nucleus, Hac1 binds by dimerization to the UPRE element found in many promoters coding for proteins of the folding machinery. By deciphering the activation mechanism of the pathway, it came as a surprise that Ire1 splices Hac1 mRNA, by an unconventional splicing reaction [41]. This mechanism was later found conserved in all metazoan cells. The Ire1-branch is therefore considered to be the evolutionary most ancient branch of the UPR [30].

1.6.2 The Ire1-Hac1/XBP1 Branch in Yeast and Metazoans

Ire1 is a bifunctional ER-resident membrane kinase/endoribonuclease, which constantly measures the folding of proteins within the ER lumen. A crystal structure of the luminal sensing domain and recently an *in vitro* study have elucidated that Ire1 can bind short basic peptides, thereby triggering an oligomerization of Ire1 molecules [42-44]. Oligomerization, in turn, results in trans-autophosphorylation of the cytosolic kinase domain, providing the means by which the signal is transmitted across the ER membrane [45]. Activated Ire1 acts as a site-specific endoribonuclease, cleaving the mRNA encoding the transcription activator Hac1 at two discrete positions, and removing a 252-nucleotide nonclassical intron [46,47]. A second enzyme, tRNA ligase (Rlg1), then joins the severed exons to produce a spliced version of Hac1 mRNA, termed Hac1i mRNA (i for UPR-induced) [41]. The Hac1 mRNA splicing reaction mediated by Ire1 and Rlg1 is completely spliceosome-independent, and utilizes chemistry that closely resembles pre-tRNA splicing. In detail, Ire1-RNase produces 2',3'-cyclic phosphates at the 3' end of RNAs, which then are recognized by the tRNA ligase [47]. In the unspliced Hac1 mRNA, the intron forms a long-range base-pairing interaction with its

5' untranslated region (UTR), which prevents ribosome initiation and therefore Hac1s translation [48]. Upon ER stress, splicing abolishes translational inhibition, allowing production of the Hac1 transcription factor. In metazoans, activated Ire1 cleaves the XBP1 mRNA at two discrete stem-loop structures, excising a 26bp short intron [49]. The two severed exons are then ligated to produce spliced XBP1 mRNA, which because to a frame-shift induced by the splicing event, are translated to produce active XBP1 [50]. The enzyme(s) involved in the ligation reaction of the two exons of XBP1 are yet to be discovered in mammalian cells.

Several studies have defined the transcriptional scope of the mediated Ire1-Hac/XBP1 branch. For instance, in yeast Hac1 activates more than 350 genes (5% of the genome), which was much larger than anticipated [31]. Targets include genes encoding for proteins involved in ER protein folding, modifications, phospholipid synthesis, ERAD, and vesicular transport in the secretory pathway downstream of the ER. Most of these genes are bearing an activating sequence in their promoter region called UPRE-1, -2 and -3, to which Hac1 binds. Activated XBP1 transcriptional factor shows a similar scope of targets in metazoans [51].

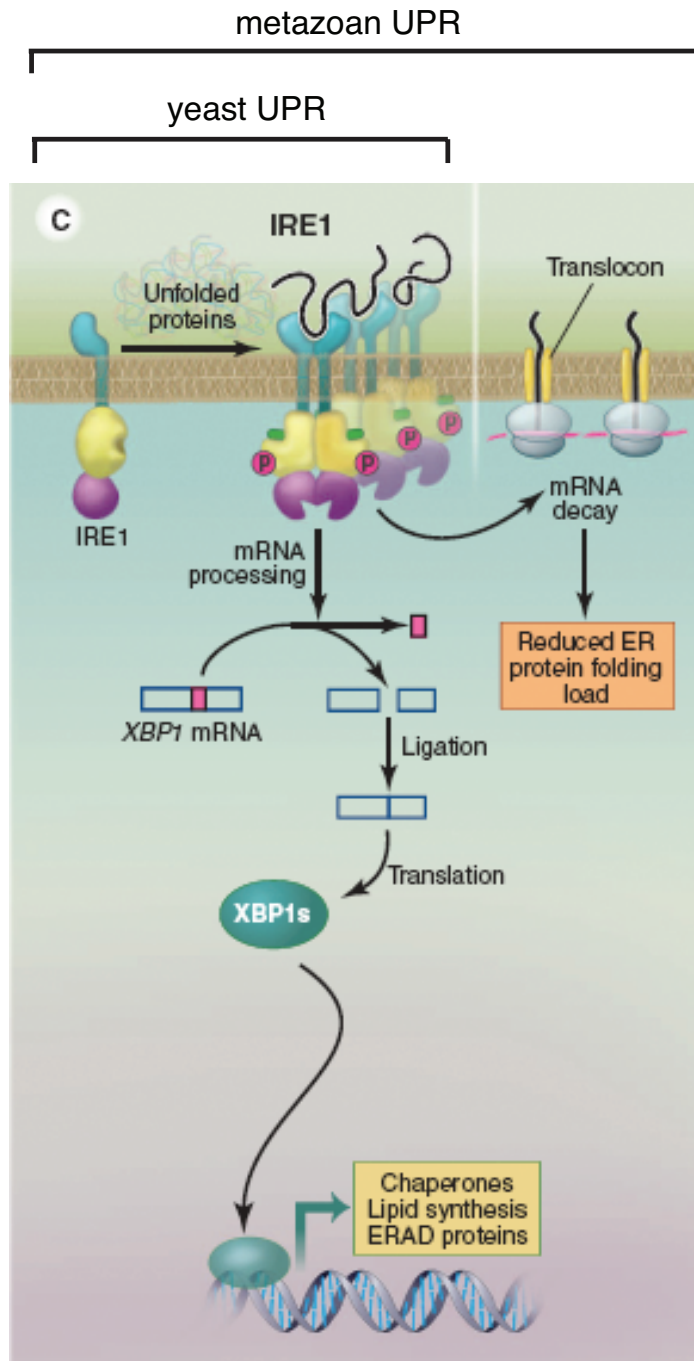


Figure 1. Ire1 signaling in yeast and metazoans

In yeast and metazoans Ire1 senses levels of unfolded proteins in the ER lumen and communicates this information across the membrane to activate a bZIP transcription factor, Hac1 (in yeast) or XBP1 (in metazoans) via an unconventional splicing reaction. Once activated Hac1/XBP1 travels to the nucleus and induces transcription of its target genes.

Restricted to metazoans: Ire1 initiates decay of ER-targeted mRNAs, a process called RIDD to reduce the load into the ER (adapted from Walter and Ron, 2011)

1.6.3 PERK and ATF6, Two Additional UPR Branches in Metazoans

In metazoan cells two additional ER-resident transmembrane sensors, are present: PERK and ATF6 which transmit information into the cytosol, each activating transcription factors that collaborate to drive expression of UPR target genes. Therefore the UPR is a network of evolutionarily conserved signal transduction pathways that monitors the conditions in the ER lumen to induce a transcriptional response [30].

The ER stress transducer PERK (double stranded RNA-activated protein kinase) is a type I transmembrane protein with a kinase domain on its cytosolic site [52]. Interestingly, the ER luminal site of PERK superficially resembles Ire1 [53]. In particular, Ire1 operates in parallel with PERK, bearing homologous luminal domains that are experimentally interchangeable, suggesting they have similar mechanisms of sensing folding in the ER. When activated, PERK phosphorylates itself and the alpha-subunit of eukaryotic translation initiation factor-2 (eIF2 α) at serine 51, which impairs global translation initiation [54]. Two consequences arise from this regulatory step: first, the mRNA translation is tuned down, and the load of proteins entering the ER is reduced. This beneficially contributes to the rebalancing of the ER. Second, mRNAs containing small upstream open reading frames (uORFs) in their 5' untranslated region are preferentially translated under conditions where translation initiation is limiting, allowing translation of the transcription factor ATF4.

metazoan UPR

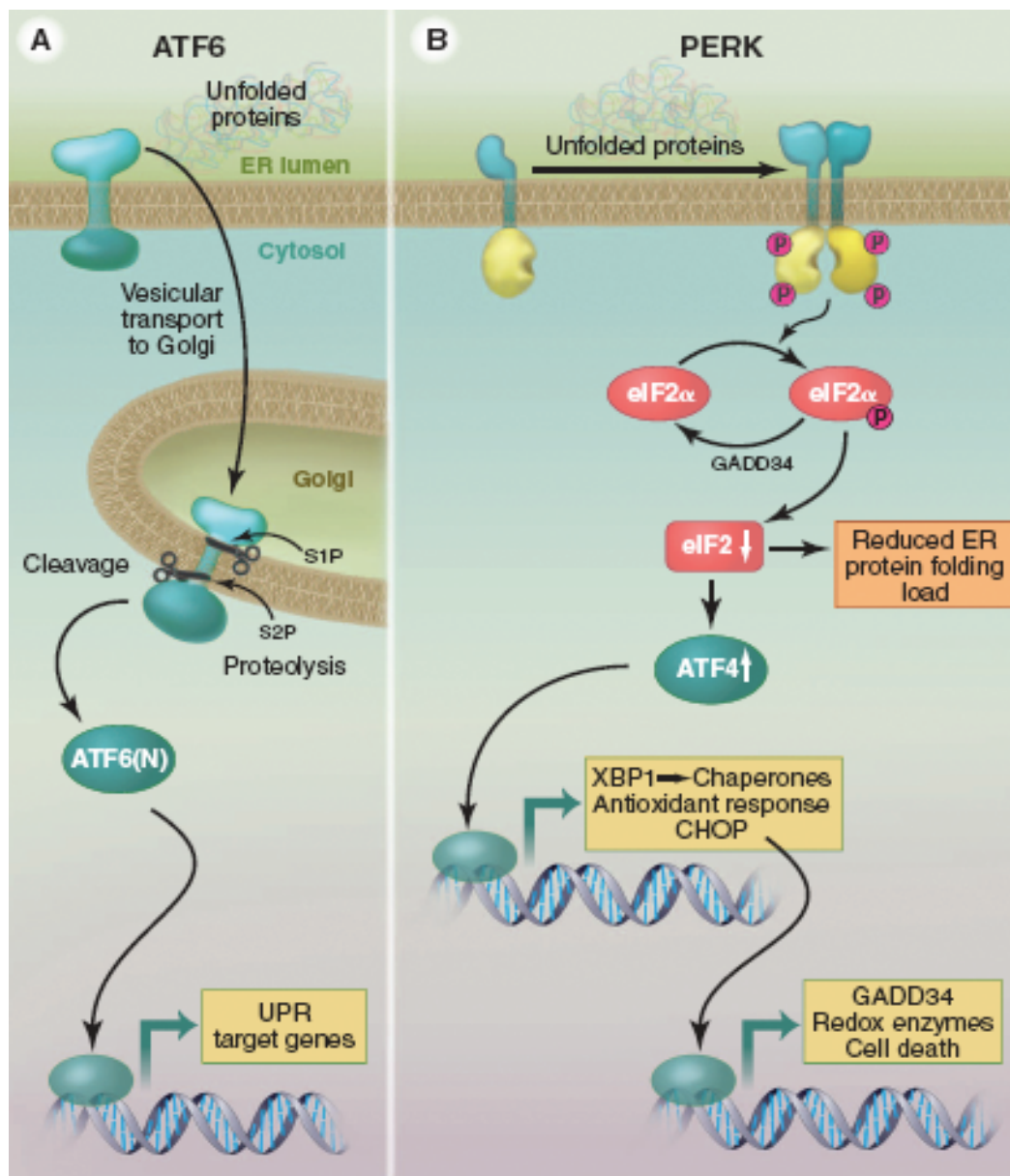


Figure 2. ATF6 and PERK signaling in metazoans

In unstressed conditions ATF6 resides in the ER membrane. Upon ER stress ATF6 transits to the Golgi apparatus. In the Golgi ATF6 is subjected to a consecutive cleavage by two proteases S1 and S2, liberating the cytosolic portion, which includes a transcription factor and allows traveling to the nucleus to bind UPR target genes. PERK senses levels of unfolded proteins by a similar mechanism as Ire1 in the ER lumen and communicates this information across the membrane to phosphorylate eIF2 α and reducing translation initiation to decrease the protein load in to the ER. Translation inhibition activates ATF4, which targets CHOP and GADD34 (adapted from Walter and Ron, 2011).

Two important gene targets of ATF4 are CHOP (transcription factor C/EBP homologous protein) and GADD34 (growth arrest and DNA-damage inducible 34). CHOP, representing another transcription factor, controls genes encoding components of the apoptosis machinery [55]. Therefore, PERK signaling has opposed consequences for cells. On one hand it decreases the flux into the ER mediating a cytoprotective response, while on the other hand CHOP activation through ATF4 contributes to cell death upon UPR induction [30]. The dualism is likely to be regulated at the level of eIF2 α phosphorylation. GADD34 encodes a PERK-inducible regulatory subunit of the protein phosphatase PP1C that counteracts PERK by dephosphorylating eIF2 α [56]. Therefore, GADD34 establishes an essential negative feedback regulation of eIF2 α , since prolonged translation inhibition is lethal for every eukaryotic cell (see Figure 2).

ATF6, signaling in the third branch of the UPR, is a transcription factor that is made as an ER-resident transmembrane protein. Upon accumulation of unfolded proteins, ATF6 is activated (by a mechanism yet to be discovered) packed into vesicles and transported to the Golgi apparatus [57]. There, ATF6 is sequentially cleaved by two proteases (S1 and S2), releasing its cytosolic N-terminal domain, which when severed from its membrane tethers functions as a bona fide bZIP transcription factor. Cleaved ATF6 can collaborate with XBP1 inducing a UPR transcriptional response, mainly to upregulate the ER folding machinery (also see Fig 2). By using the identical proteases, ATF6 processing resembles the mechanism by which the sterol response element binding protein (SREBP) is activated that controls sterol biosynthesis in mammalian cells [58].

1.6.4 Post-transcriptional Output of the UPR

Thus by first approximation, the three metazoan UPR branches collaborate to effect comprehensive transcriptional outputs, thereby enhancing the capacity of the ER according to need. As described before, PERK superimposes another layer of control by reducing the load of proteins entering the ER through translation inhibition [52].

Similarly, Ire1 is thought to play a dual role in UPR regulation in metazoans. In particular, Hollen and Weissman discovered in *Drosophila* cells that Ire1 induction not only results in splicing of XBP1 mRNA, but also mediates enhanced mRNA breakdown [59,60]. This output of Ire1 RNase activation, termed “regulated Ire1-dependent decay”, or “RIDDC”, is conserved

in mammalian cells, but not in *S. cerevisiae* and other yeast species where transcriptional control via HAC1 mRNA splicing remains the only known route of UPR signaling [61]. Therefore, it is thought that the event only occurs in metazoans. All identified RIDD target mRNAs are translated by membrane-bound ribosomes at the ER surface, where they are cleaved, most likely by Ire1 directly. Once nicked and no longer protected by their poly(A) tails and 5' caps, mRNA fragments are quickly degraded by the RNA surveillance machinery [59,62].

By contrast to the strictly conserved stem/loop structures found at XBP1/HAC1 mRNA splice sites, RIDD target mRNAs do not contain easily recognizable features in common [42,47]. Consequently, RIDD is thought to arise by a more promiscuous cleavage mode of Ire1. It is unclear whether RIDD is mediated by a unique conformation of activated Ire1, or whether it simply arises in a high-order Ire1 oligomerization state, which may serve to locally enhance low affinity interactions through avidity effects. RIDD cleavage reactions have been reconstituted in vitro with recombinantly expressed purified Ire1, lending support to the notion that Ire1's endoribonuclease activity, rather than another enzyme recruited to it, carries out the initial cleavage reaction [63,64].

Because of Ire1's dual output, the physiological consequences of RIDD have been difficult to decipher. RIDD has been suggested to play cytoprotective roles, such as contributing to important feedback control on proinsulin expression in pancreatic beta-cells or protecting liver cells from acetaminophen toxicity by degrading the mRNAs encoding the cytochrome P450 variants responsible for the drug's toxification [65,66]. RIDD has also been suggested to play cytotoxic roles as a major contributor driving cells into apoptosis after prolonged and unmitigated exposure to ER stress [67,68].

Surprisingly, in the following work presented here we found no evidence that Ire1 controls transcription in the UPR of *Schizosaccharomyces pombe*. Instead, in *S. pombe* Ire1 maintains ER homeostasis through two post-transcriptional mechanisms: it initiates RIDD of a large, select set of ER-targeted mRNAs and processes *Bip1* mRNA in an unprecedented way, thereby stabilizing it. Our studies reveal an unforeseen evolutionary plasticity in maintaining ER homeostasis.

2. Results

2.1 Ire1 Down-Regulates Select mRNAs upon ER Stress

2.1.1 The Ire1-Hac1 Branch is not Conserved in Fission Yeast

UPR induction in all eukaryotic cells analyzed to date involves the Ire1-mediated, non-conventional splicing of *Hac1/XBP1* mRNA. The splice sites at which Ire1 cleaves the mRNA to initiate splicing lie in well-conserved stem/loop structures that are readily identified [47]. Moreover, the Hac1/XBP1 transcription factors are well conserved between species and easily recognized by sequence alignment among the superfamily of bZIP transcription factors (Fig 3).

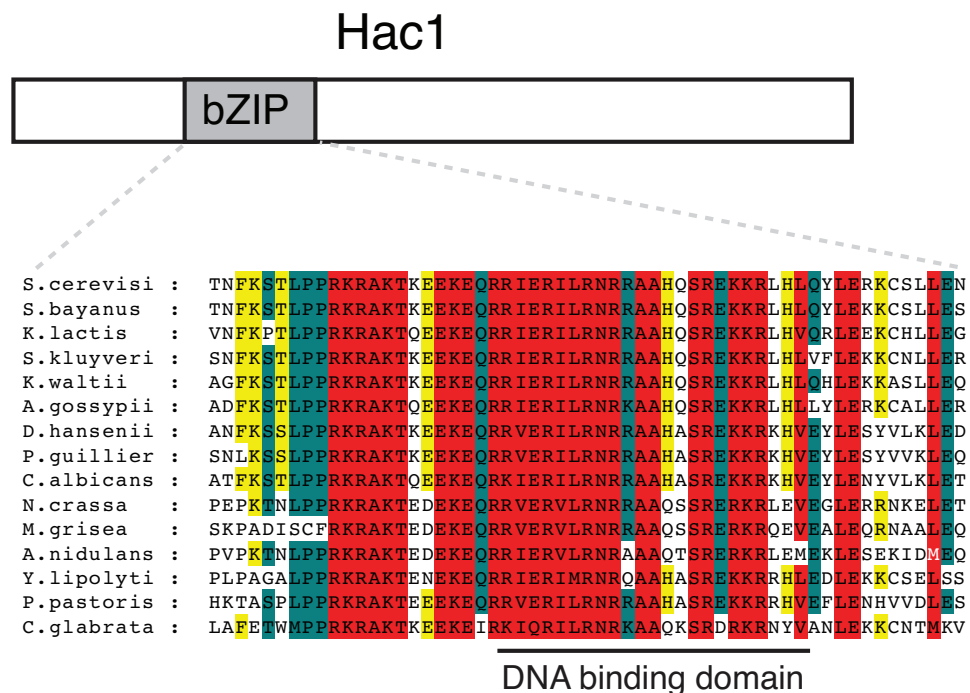


Figure 3. Alignment of DNA binding domain of Hac1 (bZIP) homologues in different yeast species. Sequence alignment was revealed by using the software ClustalW.

It was surprising that bioinformatic analyses searching for conserved stem loop structures, including loop motif *CNGNNGC*; and conserved bZIP domain failed to identify Hac1/XBP1 orthologs in *S. pombe* and other yeasts of the same genus (Fig. 4) [69,70].

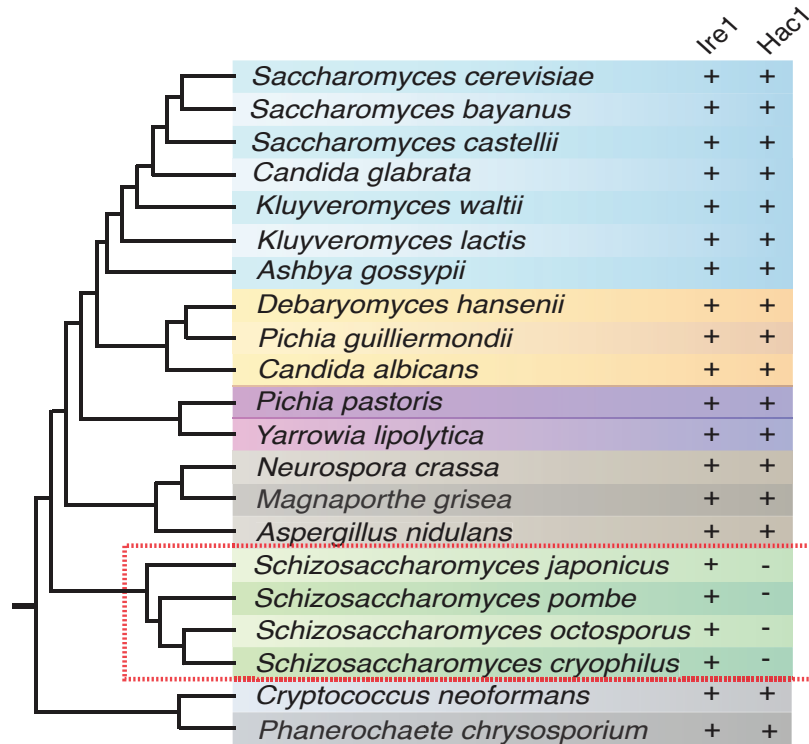


Figure 4. Presence of UPR components in different yeast species.

Phylogenetic tree showing the Ire1-Hac1 branch of the UPR in yeasts. The presence of recognizable orthologs of Ire1 and Hac1 is indicated.

2.1.2 Ire1 is Essential to Cope with ER Stress

By contrast, Ire1 is well conserved in *S. pombe*, with all of the functionally important hallmarks identified in other eukaryotes, including its ER luminal unfolded protein sensing domain and its cytosolic kinase and RNase domains. To testify that Ire1 is important to cope with ER stress, Ire1 was defected by homologous recombination. By performing a spot assay, it was observed that Ire1 was essential for *S. pombe* growth on tunicamycin (Tm) (Fig.5). Tunicamycin induces ER stress by blocking *N*-linked glycosylation, indicating that Ire1 serves an essential function in allowing cells to cope with ER stress. In all cells, Ire1 mediates signaling by activating its RNase domain. To decipher Ire1 RNase importance here, a catalytic histidine (H1018N) in the active center of Ire1 RNase was mutated, which has been shown in earlier studies to prevent RNase activity while not disrupting RNA binding (“RNase dead mutant”). Wild type Ire1 was substituted against an Ire1 RNase mutant by a pop-in-pop

selection method. Indeed, *Ire1(H1018N)* carrying this single amino acid substitution of a catalytic residue in Ire1's RNase active site preventing enzymatic activity site failed to support cell growth on tunicamycin (Fig. 5). These results established a functional UPR and the importance of Ire1 RNase activity to cope with ER stress in fission yeast.

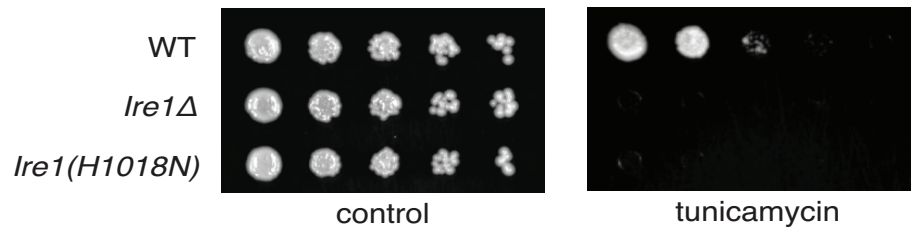


Figure 5. Ire1 is essential on ER stress in fission yeast.

Spot assay by serial dilution of wild type, *Ire1Δ* and *Ire1(H1018N)* cells spotted on solid media with or without 0.03 $\mu\text{g/ml}$ of the ER stress inducer tunicamycin (Tm). Plates were photographed after 3 days of growth at 30°C.

2.1.3 ER Stress-dependent mRNA Down-Regulation

Deep-sequencing library was prepared in collaboration with Marcy Diaz. I did data analyses and discovered mRNA down-regulation.

To address the conundrum posed by the missing Ire1 splicing substrate Hac1 in *S. pombe*, it was first explored the scope of UPR-dependent changes in gene expression. In all eukaryotic cells Ire1 activates a comprehensive transcriptional program, for instance in *S. cerevisiae* more than 5% of the genome. To this end, polyA⁺ RNA was isolated from wild type and *Ire1Δ* cells, in which the UPR was induced with the reducing agent dithiothreitol (DTT). DTT causes ER stress by impairing disulfide bond formation in the ER. The purified mRNA population was reverse-transcribed and subjected to deep-sequencing. Unexpectedly, it was observed widespread Ire1-dependent mRNA down-regulation, but virtually no mRNA up-regulation (Fig. 6). Thirty-nine mRNA species were reduced by more than two-fold in a DTT- and Ire1-dependent manner (Fig. 6 bottom left grayed area). Intriguingly, the set of down-regulated genes exclusively encoded proteins targeted to the ER (identified by signal sequences and/or transmembrane segments) (Fig. 6, red circles).

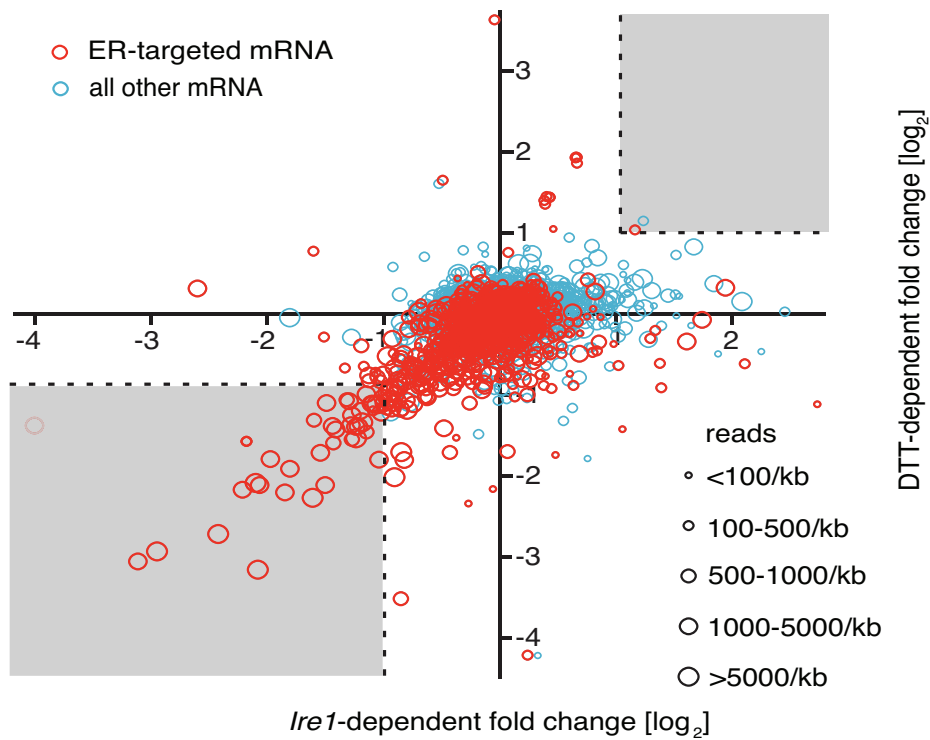


Figure 6. Genome-wide Ire1- and DTT-dependent gene expression profile by polyA⁺ selection.

Strand-specific polyA⁺ enriched mRNA-Seq analysis of annotated ORFs. The plot indicates the fold change (\log_2) of transcript abundance in DTT-stressed *Ire1Δ* cells (2 mM DTT, 1 h) compared to DTT-stressed wild type cells (2 mM DTT, 1 h) in the x-axis, and transcript abundance in unstressed wild type cells compared to DTT-stressed wild type cells (2 mM DTT, 1h) in the y-axis. Symbol sizes indicate abundance classes for each mRNA (reads per kilobase). Transcripts encoding proteins with a signal sequence or transmembrane segment are colored red, all other transcripts are colored blue

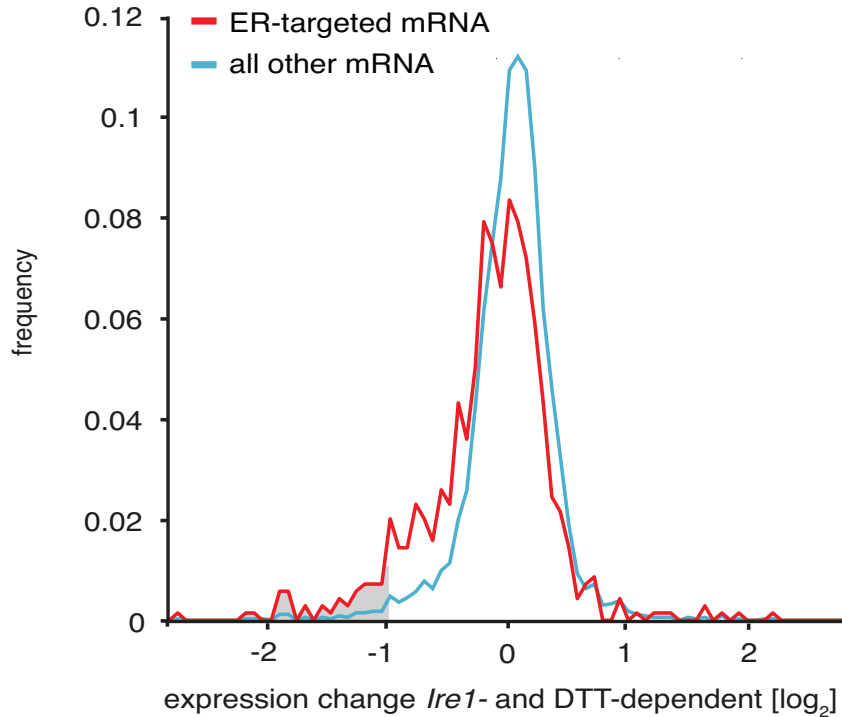


Figure 7. Genome-wide Ire1- and DTT-dependent gene expression.

B. DTT-dependent and Ire1-dependent expression changes of transcripts displaying a signal sequence or a transmembrane domain. The skew of the left tail of the distribution indicates an enrichment ($P < 1 \times 10^{-20}$) of down-regulated mRNAs. Coloring is as in **A**.

As shown in Figure 7, the genome-wide profile of Ire1- and ER stress-dependent mRNA changes of genes encoding ER-targeted proteins is skewed to a significantly greater extent towards down-regulation than that of other mRNAs ($P < 1 \times 10^{-20}$). An obvious reason to be preferentially down-regulated by Ire1 could be the abundance of each mRNAs. Most members of this set of down-regulated mRNAs were abundantly expressed, as depicted by the size of the plotted circles in Figure 6. However, when plotting abundance mRNAs versus fold-change upon ER stress, the down-regulation did not correlate with mRNA abundance as shown in Figure 8.

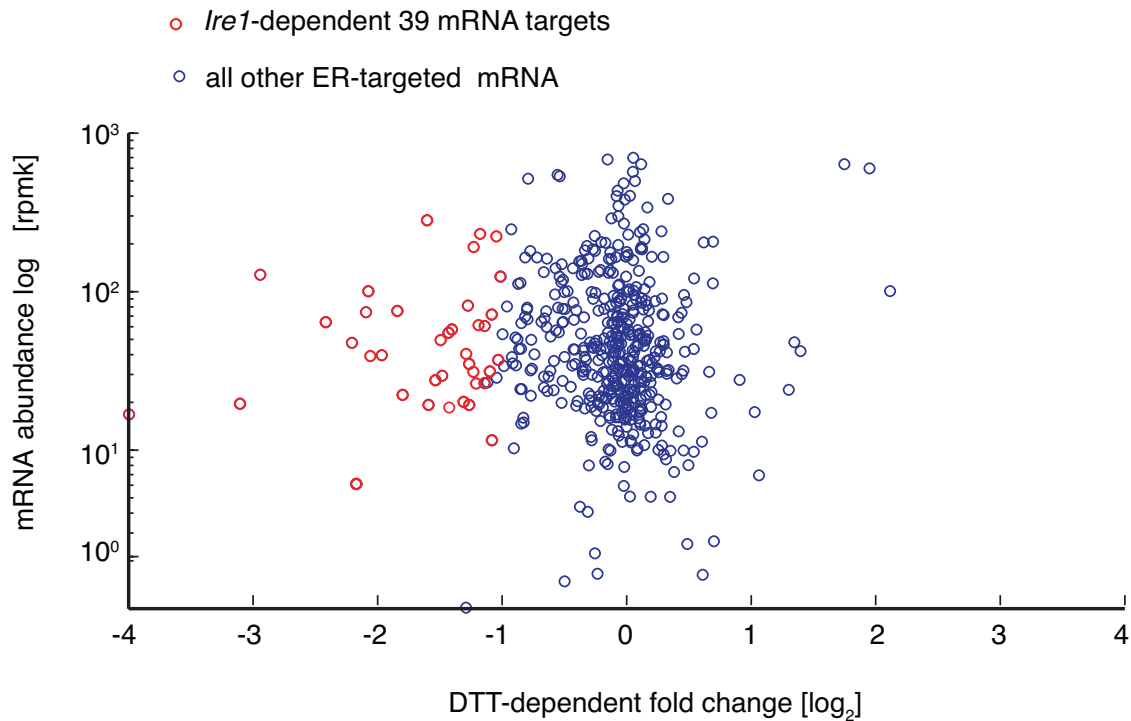


Figure 8. mRNA abundance versus DTT-dependent expression fold change
 Plot depicting ER-targeted mRNAs abundance [\log_{10}] (reads per million) versus DTT-dependent expression changes [\log_2] for wild type cells.

2.1.4 Gene-Ontology Analysis of Down-Regulated mRNAs

GO analysis of the 39 target mRNAs revealed that more than half of the most down-regulated mRNAs encode proteins with annotated functions in the secretory pathway, in particular proteins involved in lipid metabolism, trafficking, and ER functions (Fig. 9).

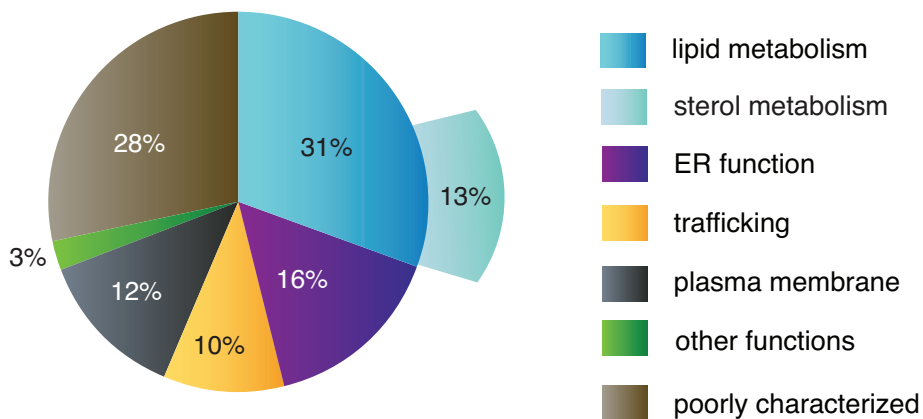


Figure 9. Distribution of gene-ontology (GO) annotations for Ire1-dependent down-regulated mRNAs.

Percentages indicate genes within a particular GO category in relation to the total number of genes that have a GO annotation (N = 39).

2.1.5 Ire1 Down-Regulates mRNAs Encoding Ergosterol Biosynthesis

Proteins

The mRNA down-regulation of sterol metabolism enzymes were particular intriguing to us. Mapping the precise position of each down-regulated mRNA within the ergosterol biosynthesis pathway (see Fig. 10) revealed an enrichment of mRNA targets at the end of the synthesis pathway. In general, sterol levels are sensed and regulated by SREBP (note: *S. cerevisiae* lacks a homolog), an ER-transmembrane transcription factor, which induces upon sterol depletion an expression program to produce more sterol synthesis enzymes [71,72].

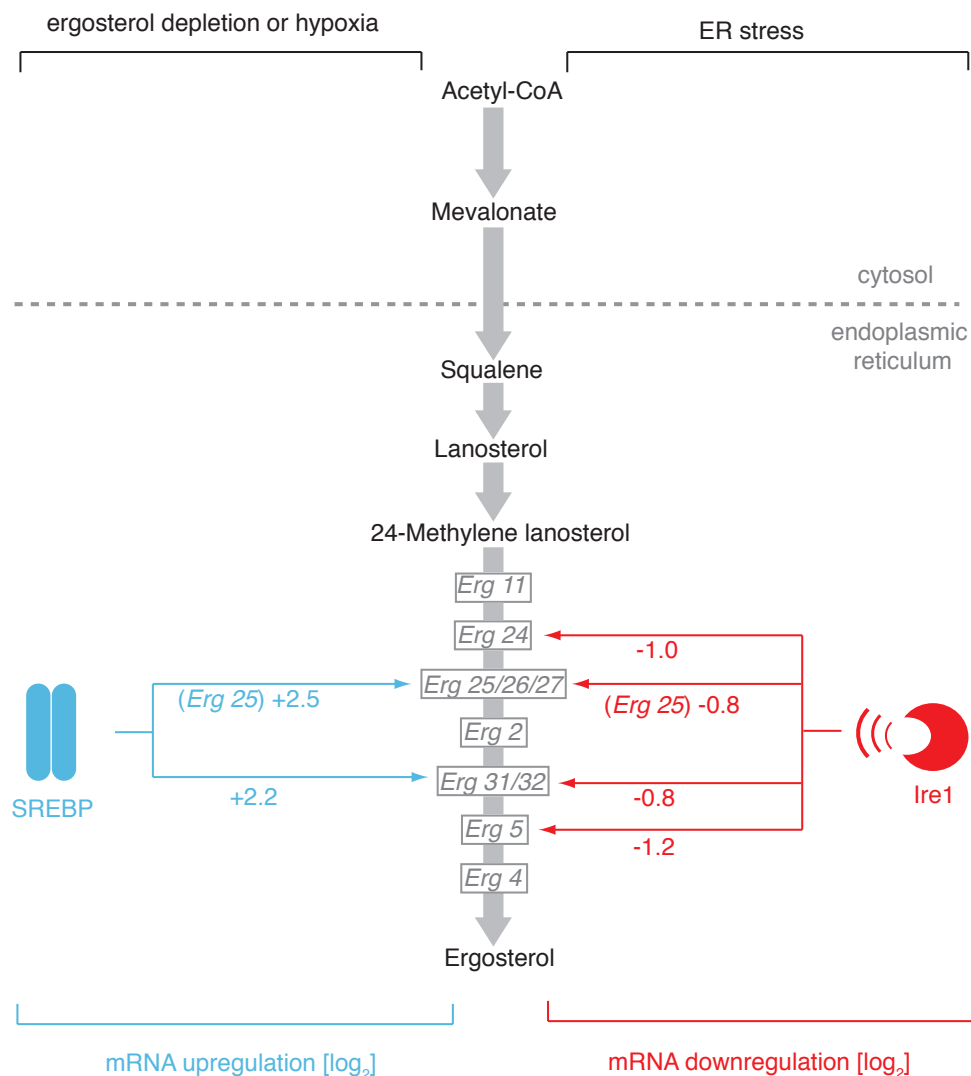


Figure 10. SREBP- and Ire1-regulated steps in ergosterol synthesis pathway in *S. pombe*. SREBP data are revealed from Hughes, et al 2005; Ire1-dependent data are from this study.

It is worth noting here, that SREBP- and Ire1-targets are partially overlapping, but regulated with an opposed outcome.

Studies in mammalian cells have shown that an abnormal sterol accumulation is toxic. For instance, feeding macrophages with external cholesterol depleted the calcium store in the ER, induced ER stress and triggered cell death [73]. In conclusion, this and other studies revealed that abnormal levels of lipids and cholesterol cause ER stress, inducing a massive UPR response [74]. Therefore, a selective Ire1-dependent disruption of ergosterol synthesis could benefit cells to cope with ER stress here in fission yeast. As seen in figure 10, *Erg5* mRNA-encoding the second-last step in ergosterol biosynthesis - decreases more than 2 fold in an Ire1- and DTT-dependent manner. To this end, *Erg5* was deleted to mimic a more drastic and permanent down-regulation of ergosterol synthesis under ER stress. By performing a spot assay, *Erg5* deleted cells grow significantly better than wild type cells, supporting the hypothesis of beneficial adjustment of sterol levels by Ire1 (Fig. 11).

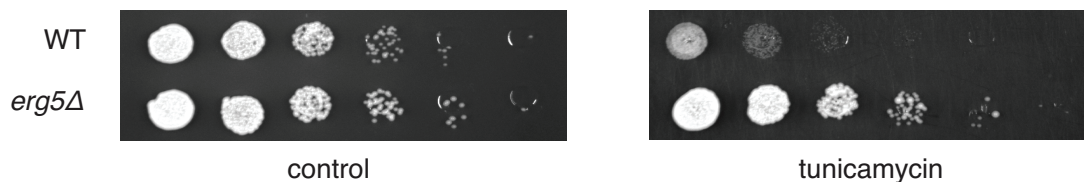


Figure 11. *Erg5* deletion is beneficial for cell growth upon ER stress.

Spot assay by serial dilution of wild type, *Ire1Δ* and *Ire1(H1018N)* cells spotted on solid media with or without 0.03 $\mu\text{g/ml}$ of the ER stress inducer tunicamycin (Tm). Plates were photographed after 3 days of growth at 30°C.

In the future, it has to be shown for instance by lipidomic analysis of these cells, that indeed Ire1 induces an ergosterol decrease. Moreover, the precise molecular advantage of decreased sterol levels under ER stress is still rudimentary and has to be elucidated.

2.1.6 Ire1 Cleaves Down-Regulated mRNAs at Specific Sites

I chose the mRNA candidates. Marcy Diaz did the deletion of the cytosolic mRNA machinery. Northern blot analysis was performed in collaboration with Marcy Diaz.

As the reduction in mRNA abundance was ER stress- and Ire1-dependent, it was explored if Ire1 could be directly involved in destabilizing ER-bound mRNAs. In general, endoribonucleases are cleaving mRNAs, generating two RNA fragments, which are rapidly removed by the degradation machinery. By blocking one of these cytosolic degradation pathways, cleavage products are stabilized and therefore become visible. To this end, we sought to trap any putative primary Ire1-cleavage 5' products prior to degradation by deleting *Ski2*, which encodes a helicase component of the cytosolic Ski complex (cytosolic exosome) that mediates 3' → 5' RNA decay. Northern blot analysis of *Ski2Δ* cells revealed that *Gas2* mRNA (which is down-regulated 2.5-fold in an ER stress and Ire1-dependent manner) yielded two discrete cleavage products upon ER stress (Fig. 12A * and ▲). *Gas2* mRNA cleavage was dependent on Ire1, as no mRNA reduction and no cleavage products were observed in *Ire1Δ Ski2Δ* double deletion cells (Fig. 12A). Another target, *Yop1*, behaved similarly (Fig. 12B).

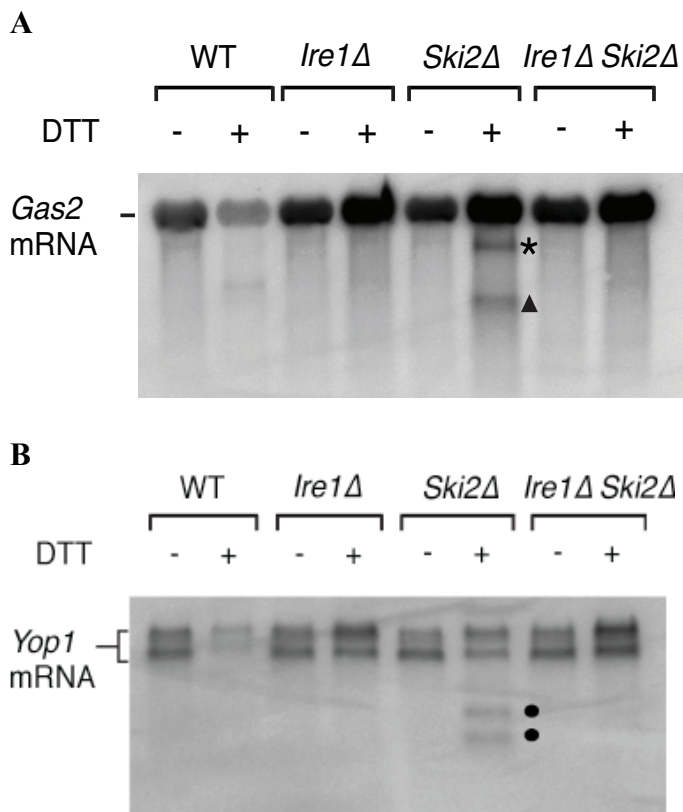


Figure 12. Visualizing cleavage products of *Gas2* and *Yop1* upon ER stress

A. Northern blot of total RNA extracted from wild type, *Ire1Δ*, *Ski2Δ* and double mutant ER stressed *Ire1Δ Ski2Δ* cells (2 mM DTT, 1 h). A probe complementary to the 5' UTR of *Gas2* was used to detect cleavage products. The triangle and asterisk indicate two different mRNA cleavage products.

B. Northern blot of total RNA isolated from wild type, *Ire1Δ*, *Ski2Δ* and double mutant *Ire1Δ Ski2Δ* ER stressed cells (2 mM DTT, 1 h). A probe complementary to the 5' UTR of *Yop1* was used to detect cleavage products. The dots indicate Ire1-dependent mRNA cleavage products.

2.1.7 Importance of the 3'->5' mRNA Degradation Machinery to Cope with ER Stress

In time-course experiments, reduction of *Gas2* mRNA and accumulation of the cleavage products peaked at 30 min after UPR induction (Fig. 13b); at later time points the abundance of intact full-length mRNA increased (see figure 12 after 60 min), suggesting that newly transcribed mRNA is not cleaved if the Ire1-dependent cleavage products are not further degraded.

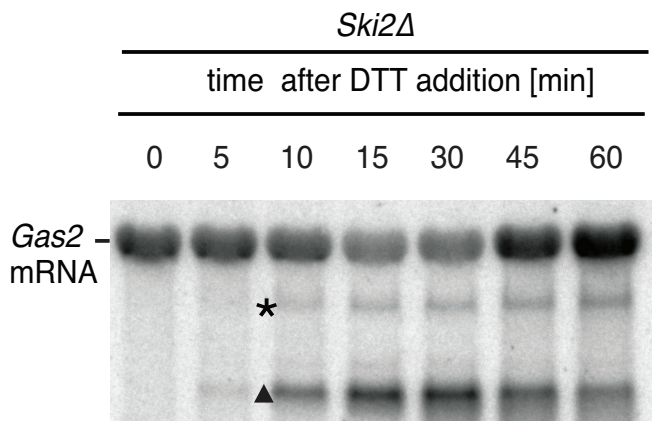


Figure 13. Time-course analysis of *Gas2* mRNA upon ER stress

Northern blot of total RNA extracted from ER-stressed *Ski2Δ* cells (2 mM DTT). A probe complementary to the 5' UTR of *Gas2* was used to detect cleavage products. The triangle and asterisk indicate two different mRNA cleavage products.

This phenomena is supported by the fact that, *Ski2Δ* cells failed to grow on plates containing tunicamycin (Fig. 14), indicating that an intact mRNA decay machinery is important for *S. pombe* cells to cope with ER stress.

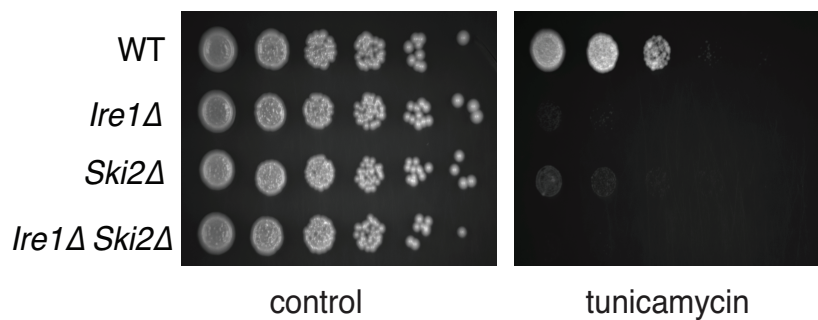


Figure 14. *Ski2* function is important on ER stress

Spot assay by serial dilution of wild type, *Ire1Δ*, *Ski2Δ* and *Ire1Δ Ski2Δ* cells spotted on solid media with or without ER stress as in Figure 5.

2.1.8 Genome-Wide Identification of Specific Ire1 Cleavage Sites

Deep-sequencing library was prepared by Marcy Diaz. Data were analyzed by me.

To determine the mRNA cleavage sites genome-wide, total RNA fractions were prepared from *Ski2Δ* and from *Ire1Δ Ski2Δ* cells where 5' fragments are stabilized. tRNA ligase was used to attach linker sequences specifically to those 5' RNA fragments terminating in a 2',3'-cyclic phosphate, which is the expected product of Ire1-catalyzed RNA cleavage [75]. Then the cleavage products were amplified in 3' RACE reactions priming at the linker sequence. Alignment of the sequencing data to the *S. pombe* genome identified the 3' ends of Ire1-dependent fragments. In particular, we identified 39 Ire1-dependent fragments mapping to 24 of the most down-regulated genes, as shown in Figure 15 for *Gas2* mRNA.

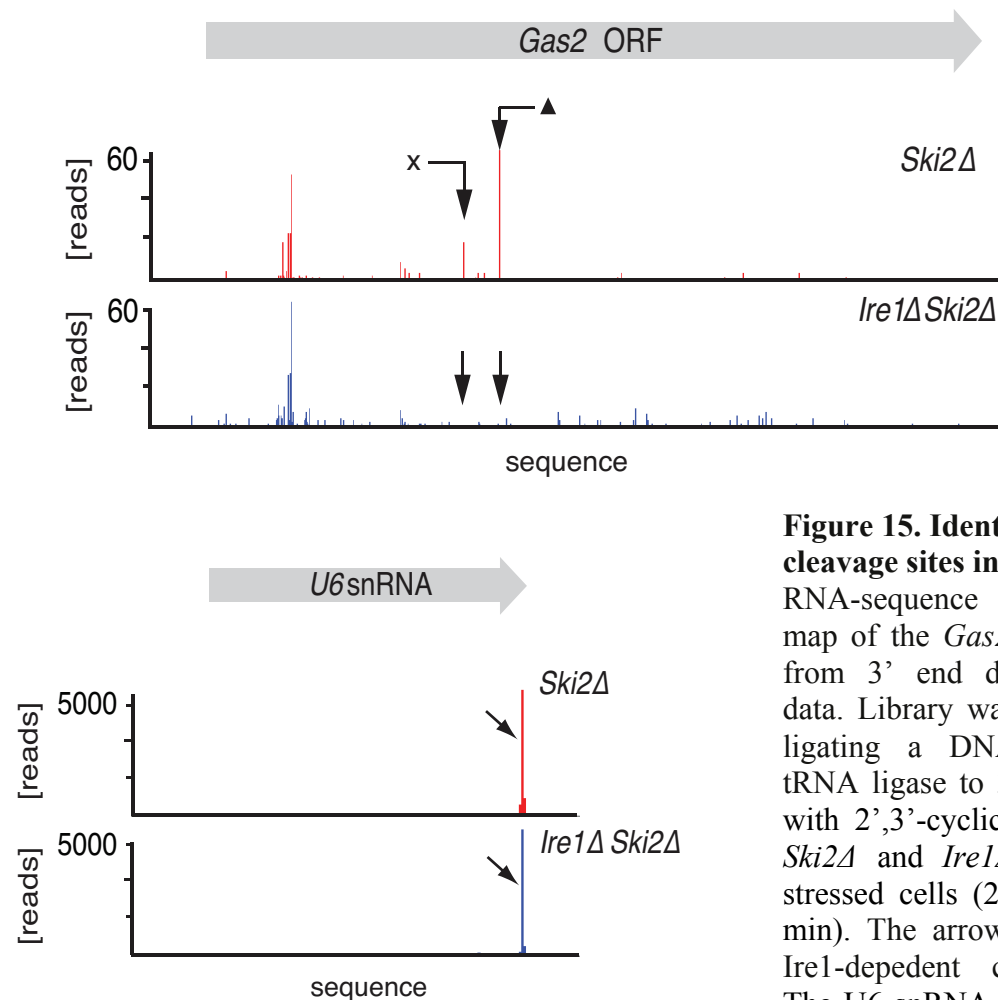


Figure 15. Identifying Ire1 cleavage sites in *Gas2* mRNA

RNA-sequence read density map of the *Gas2* locus derived from 3' end deep-sequencing data. Library was generated by ligating a DNA-linker using tRNA ligase to 3' end mRNAs with 2',3'-cyclic phosphates in *Ski2Δ* and *Ire1Δ Ski2Δ* ER-stressed cells (2 mM DTT, 30 min). The arrows indicate two Ire1-dependent cleavage sites. The U6 snRNA locus was used as a positive control.

By size estimation, the major Ire1-dependent peak corresponded to the smaller, more abundant *Gas2* mRNA cleavage product (labeled ▲ in Figs. 12 and 13). A second, less abundant short fragment was also observed in the sequencing data (labeled ✕ in Fig. 15). (Fragment ✕ was absent or below the detection limit on the Northern blot unless the primary cleavage site was mutated (see Fig. 18, discussed below). Spliceosomal U6 RNA normally terminates in a 2',3'-cyclic phosphate and thus provided a valuable control for the ligation reaction (Fig. 15, bottom panel).

Alignment of the experimentally determined Ire1-dependent cleavage sites revealed a core motif with a signature of three conserved nucleotides (UGC) that flank the Ire1-dependent cleavage sites at positions -2, -1, and +1 with an additional strong bias against G in position +2 (Fig. 16).

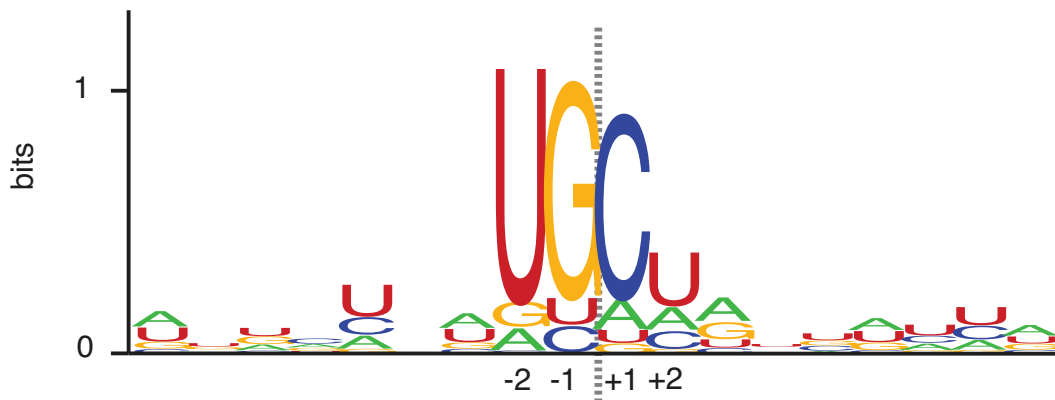


Figure 16: Ire1 RNA recognition motif

Ire1 RNA sequence recognition motifs generated by deep-sequencing analysis of tRNA ligase-generated RNA libraries of 39 mRNA targets down-regulated two fold or more in an Ire1-dependent manner. The resulting position weight matrices are illustrated as a logo. The dotted line indicates the cleavage site.

The sequence motif can be found in the splice site of XBP1, pointing to a universal conservation of this recognition motif by Ire1. Thus, most mapped mRNA cleavage sites (34 of 39), including those in *Gas2* mRNA, localized within the open reading frames.

2.1.9 ORF of *Gas2* mRNA is Sufficient to Down-Regulate mRNA

To further characterize if the information of degradation is lying in the open reading frame, and is independent from transcriptional induction, an artificial *Gas2* reporter was constructed. Indeed, a *Gas2* reporter construct transcribed off a heterologous alpha-tubulin (*Nda2*) promoter and containing only the *Gas2* ORF flanked by heterologous 5' and 3' tubulin untranslated regions (UTRs), was down-regulated upon ER stress in an Ire1-dependent manner (Fig. 17A). This degradation was quantitatively comparable to that of the native *Gas2* transcript (Fig. 17B), indicating that the information contained within the *Gas2* ORF is sufficient to confer susceptibility to Ire1-dependent cleavage.

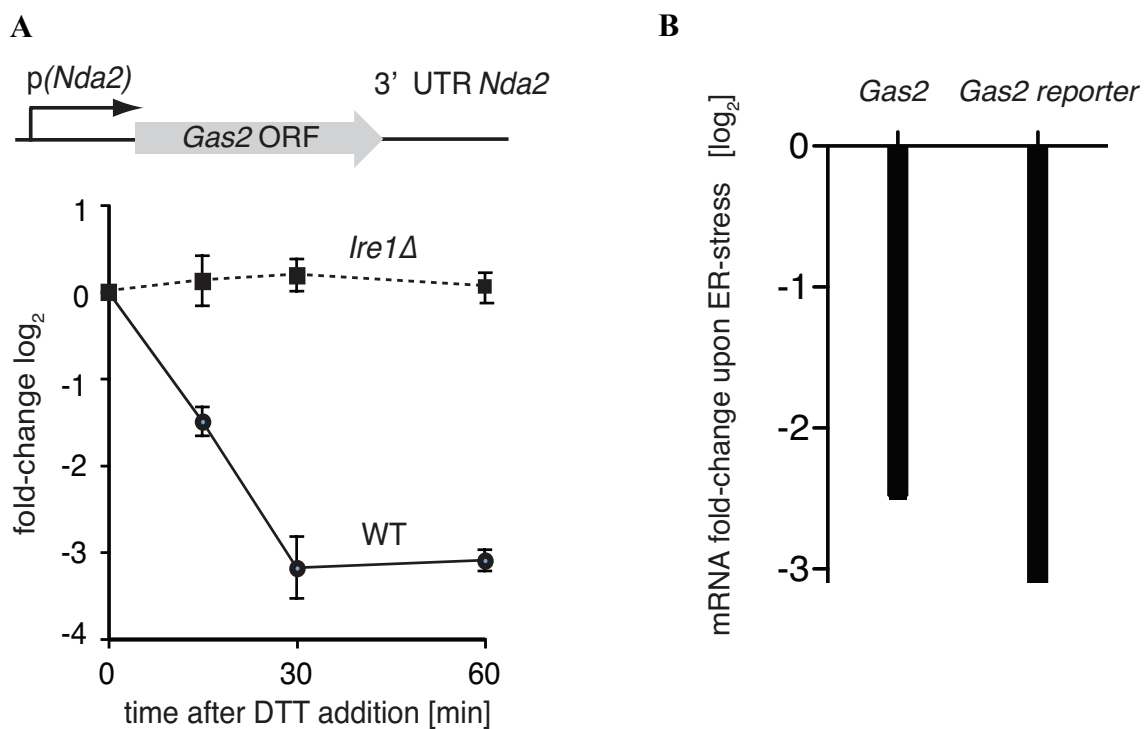


Figure 17. Time-course of the *Gas2* reporter upon ER stress

A. Real-time qPCR of a chromosomally integrated reporter containing the coding sequence of *Gas2* under the control of the *Nda2* (tubulin) promoter and including the UTRs of *Nda2*. A time course after DTT addition (2 mM) is shown. Endogenous *Nda2* was used as a normalization control. Error bars: standard deviation. **B.** Comparison of ER stress-dependent down-regulation of endogenous *Gas2* mRNA (2 mM DTT, 1 h: deep-sequencing) and reporter *Gas2* mRNA (from qPCR: 2 mM DTT, 1h; see also panel A).

2.1.10 Mutational Analysis of Ire1 Cleavage Site in *Gas2* mRNA Reporter

To assess the functional importance of the identified *Gas2* mRNA cleavage site experimentally, the UGC-residues of the ▲-site (UG\CU) were mutated. As expected, ER stress-dependent cleavage of the *Gas2* reporter mRNA at the mapped site was abolished (Fig. 18). In its place, however, two new Ire1-dependent fragments were observed (labeled ✕ and *). Scanning gel densitometry revealed that fragment ✕ is distinctly smaller than fragment ▲, and hence represents a cryptic site that is only utilized when site ▲ is mutated. Fragment * likely corresponds to the lower abundance cleavage product observed in Figures 12A and 13, which becomes more prominent in the mutant construct. Taken together, it is concluded that Ire1-dependent mRNA cleavage in *S. pombe* is sequence dependent.

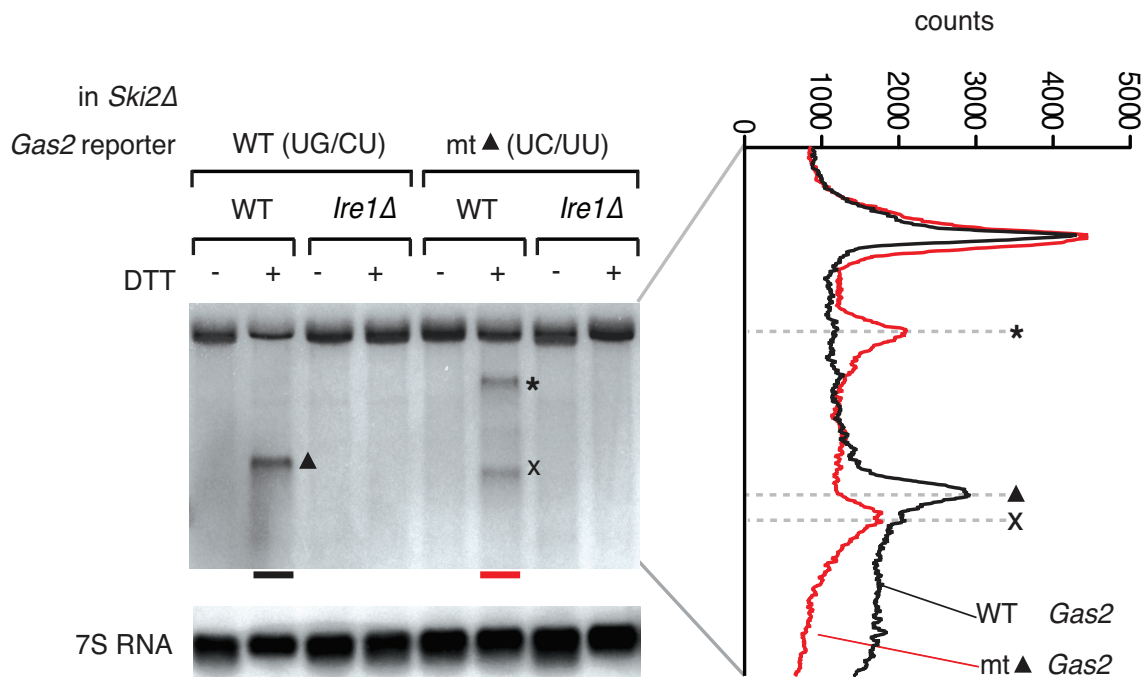


Figure 18. Mutational analysis of UG/C consensus sequence

Northern blot analysis of total RNA extracted from *Ski2Δ* and *Ire1Δ Ski2Δ* cells carrying a mutant version of the reporter indicated in 2.1.9, where the putative Ire1 cleavage site (▲, UG\CU→UC\UU) was mutated. Note that the band labeled ✕ migrates distinctly faster, as shown by scan on the right.

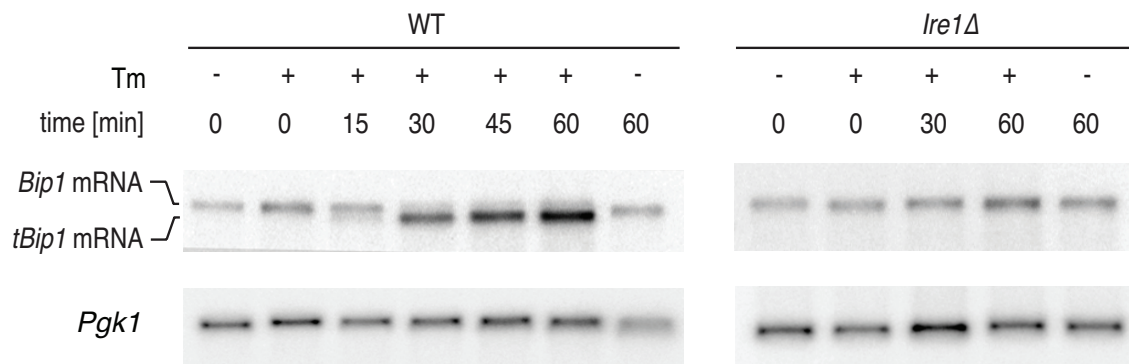
The data presented so far suggest that homeostatic control of ER protein folding is regulated differently in *S. pombe* compared to *S. cerevisiae*. Rather than relying on a transcriptional program to upregulate genes that enhance ER protein folding capacity as in *S. cerevisiae*, *S.*

pombe cells reduce the amount of specific proteins entering the organelle by decreasing the level of ER-targeted mRNAs using Ire1-dependent mRNA degradation.

2.2. *Bip1* mRNA Processing in Response to ER stress

2.2.1 *Bip1* mRNA Changes Sizes and Increases upon ER Stress

In all species analyzed to date, *Bip1* is a major UPR target gene that is up-regulated when cells experience ER stress. Paradoxically, *S. pombe Bip1* mRNA was among the 39 down-regulated mRNAs identified by the analyses shown in Figure 5. Analysis by Northern blotting yielded seemingly conflicting results: by this analysis, *Bip1* mRNA was 4-fold more abundant in ER stressed cells (Fig. 19). Intriguingly, the appearance of a faster migrating mRNA species (“*tBip1* mRNA”) indicates that *Bip1* mRNA changes size in cells experiencing ER stress (Fig. 19, lanes 3-4). The observation that *S. pombe Bip1* mRNA changes size upon ER stress dates back to 1992, but has not been further explored until now [76]. The Ire1-dependence of the *Bip1* mRNA processing upon ER stress, the molecular nature of the mRNA size shift and the physiological role are novel parts of the present work here.



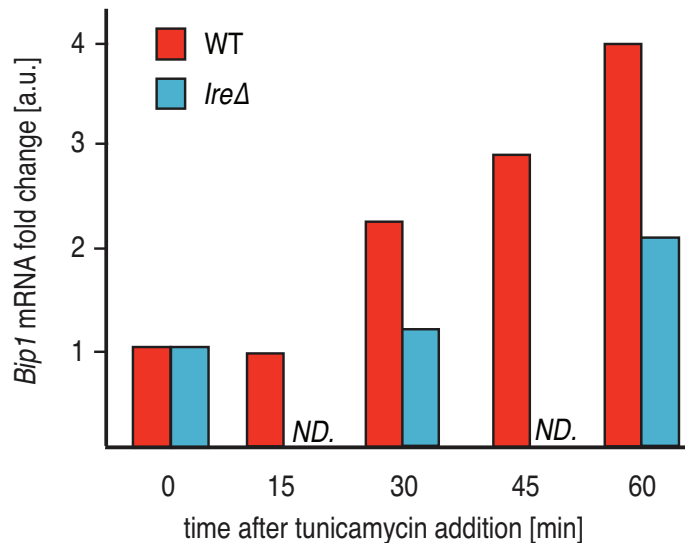


Figure 19. Time-course and quantification of *Bip1* mRNA upon ER stress

upper panel: Northern blot analysis of total RNA extracted from wild type and *Ire1Δ* cells untreated or treated with tunicamycin (1 μg/ml), and hybridized with a probe complementary to the ORF of *Bip1* mRNA. lower panel: *Bip1* mRNA quantitation normalized to *Pgk1* mRNA.

2.2.2 Increase of *Bip1* mRNA upon ER Stress Results from mRNA Stabilization

Appearance of the *tBip1* mRNA species was Ire1-dependent and in wild type cells accounted for the increase in overall mRNA abundance. This raises the question if *Bip1* mRNA is transcriptional up-regulated by an yet to be identified transcription factor. To exclude transcriptional induction of Bip1, a reporter was constructed to measure the transcriptional activity of the *Bip1* promoter. To this end, the activity of a heterologous reporter was measured in which the *Bip1* promoter was fused to GFP and showed no Ire1-dependent change in mRNA abundance with ER stress (Fig. 20). The increase did not result from augmented transcription, suggesting a post-transcriptional stabilization of *tBip1* mRNA. It shows an Ire1-independent transcriptional up-regulation, most likely caused by the heat shock element in the *Bip1* promoter.

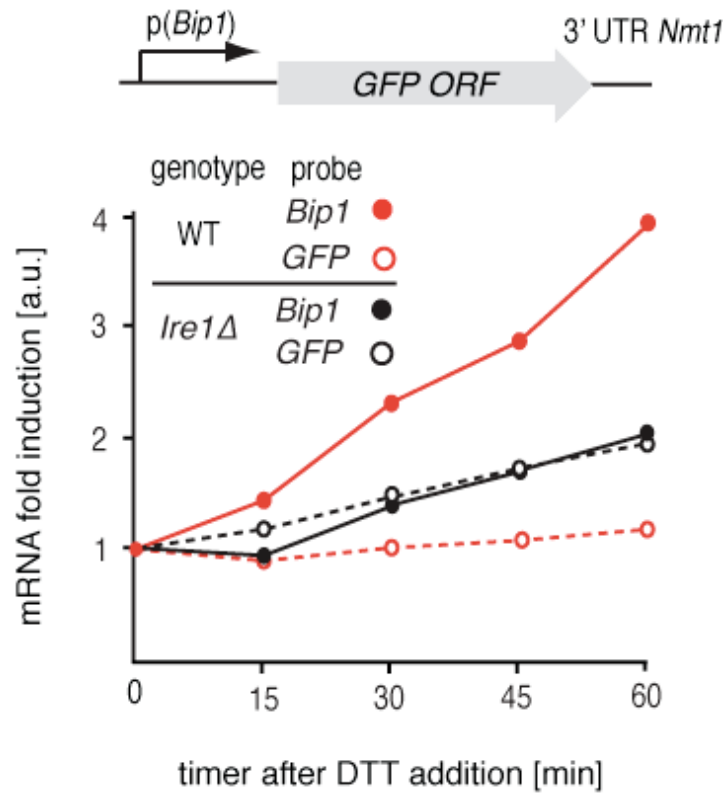


Figure 20. Transcriptional activity of *Bip1* promoter upon ER stress

The abundance of a *GFP* mRNA driven by the *Bip1* promoter (black) compared to endogenous *Bip1* mRNA was determined as a time course after DTT (2 mM) addition by quantitative Northern blotting.

Since accurate tools to determine mRNA half-lives in fission yeast are lacking, (neither RNA polymerase II temperature sensitive mutants nor transcriptional inhibitors) a transcriptional shut-off was performed. In agreement with the previous result (see Fig. 20), we found that the stability of an mRNA bearing the *Bip1* ORF and 3' UTR showed a more than 3-fold increase in half-life from $T_{1/2} = 20$ min for the unprocessed form present in unstressed cells to $T_{1/2} = 70$ min for the processed form present in ER-stressed cells (Fig. 21). Therefore, it can be concluded that the increase of *Bip1* mRNA upon ER stress results from stabilization of the mRNA.

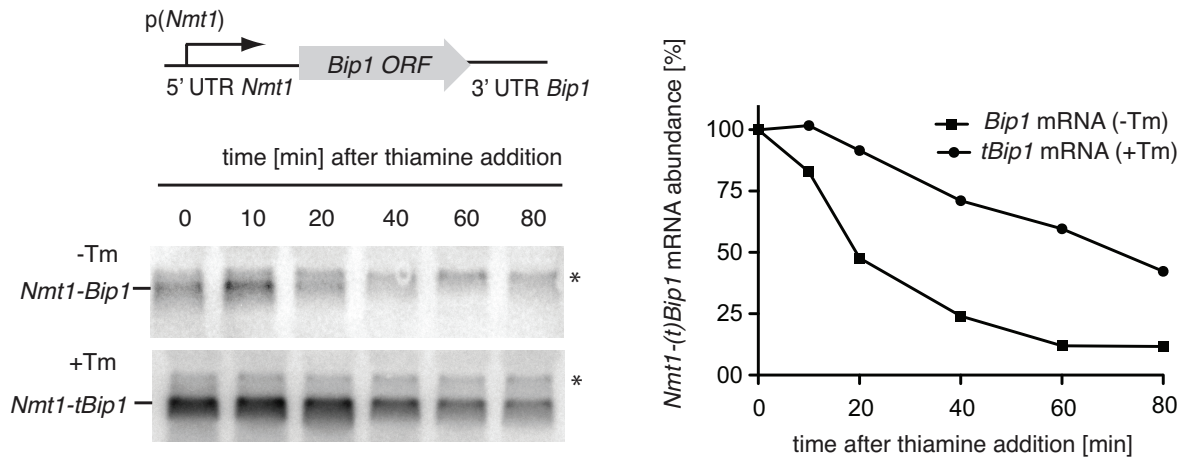


Figure 21. Half-life measurement of *Bip1* mRNA by transcription shut-off

Wild type cells bearing a construct encoding the *Nmt1* 5' UTR, *Bip1* ORF and *Bip1* 3' UTR driven by the *Nmt1* promoter were pre-treated with tunicamycin (0.25 $\mu\text{g}/\text{ml}$, 1 h). At different time points after thiamine (15 μM) addition (to effect transcriptional shut-off of the *Nmt1* promoter), RNA was extracted and analyzed by Northern hybridization. Blots were probed for the *Nmt1* 5' UTR. *Nmt1-Bip1* mRNA and *Nmt1-tBip1* mRNA were quantitated and normalized to the unspecific band (asterisk).

2.2.3 *Bip1* mRNA is Truncated in its 3' UTR upon ER Stress

Next the origin of the size shift of *Bip1* mRNA upon ER stress was explored. Sequencing of the expressed genome in UPR-induced and uninduced cells revealed the molecular difference between *Bip1* and *tBip1* mRNA (Fig. 22). For these experiments, total RNA was extracted and then, without selecting for polyA⁺ RNA, removed rRNA by subtractive hybridization. After reverse transcription, deep-sequencing of the cDNA pool from uninduced cells revealed good coverage of reads spanning the entire *Bip1* mRNA including its 5' and 3' UTR (Fig. 22, left, blue profile).

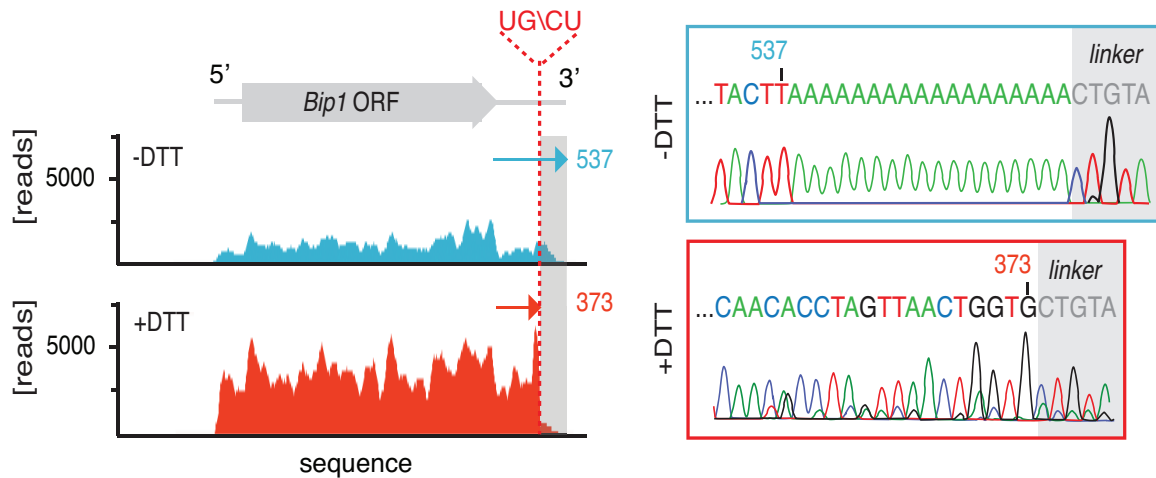


Figure 22. Sequencing map and 3' RACE of *Bip1* mRNA

RNA-sequence read density map of the *Bip1* locus derived from mRNA-enriched (ribosome depleted) RNA in wild type cells untreated or treated with DTT (2 mM DTT, 1 h; left panels). Data are representative of one of two biological replicates. Single nucleotide resolution of the 3' terminus of *Bip1* mRNA determined by 3' RACE (right panels).

Additionally, a 3'-RACE was performed to determine the exact 3' end of *tBip1* mRNA. The sequence of the amplified DNA confirmed that *tBip1* mRNA lacks a poly(A) tail and terminates at G373 in the 3' UTR (Fig. 22, right panel). In 7 independently isolated clones, no sequence variation in the *tBip1* linker junction was found. The alignment reads from the deep-sequencing data revealed a sharp ending of all truncated *Bip1* mRNA at G373 (rRNA set)

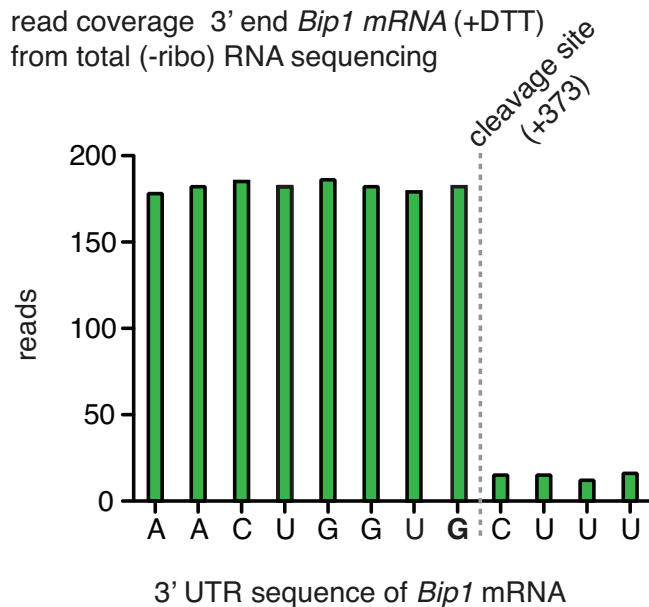


Figure 23. Single nucleotide resolution of *Bip1* mRNA 3' end upon ER stress

Sequencing read coverage of the 3' end nucleotide positions in *tBip1* mRNA derived from mRNA enriched by subtractive hybridization against rRNA (Ribominus™ kit, Invitrogen kit). Cells were treated with DTT (2 mM, 1 h).

Further, by analyzing the 3' end of *tBip1* mRNA, it was possible to align the flanking sequence with the UG\CU motif (Fig. 16), suggesting that *tBip1* mRNA is produced by truncation of *Bip1* mRNA in an Ire1-dependent RNA cleavage reaction that resembles those of the Ire1-dependent down-regulated mRNAs described above (2.1).

2.2.4 3' UTR of *Bip1* mRNA and Signal Sequence are Sufficient to Induce Truncation

Next, it was of interest to identify the minimal information to process any mRNA, like *Bip1* mRNA. The *Bip1* 3' UTR and the presence of a signal sequence were sufficient to a heterologous mRNA construct to confer Ire1-dependent processing. The dependence of correct targeting to the ER supports the idea of an Ire1-dependent cleavage.

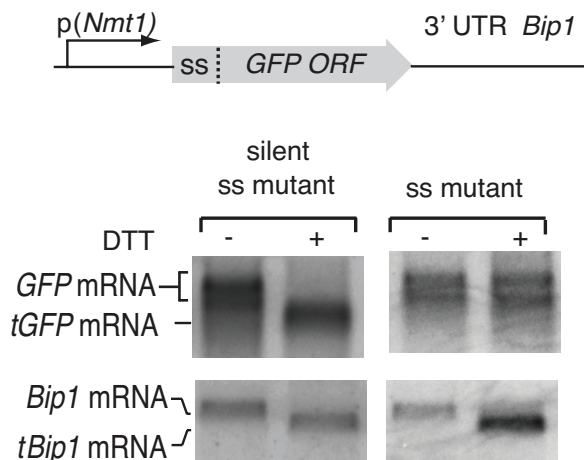


Figure 24. *Bip1* 3'UTR processing is transplantable and depends on ER targeting

Northern blot analysis of wild type cells bearing a construct expressing a RNA coding for a fusion protein of GFP preceded by the *Bip1* signal sequence. The constructs includes the *Bip1* 3' UTR. Expression was driven by the *Nmt1* promoter. Cells were untreated or treated with DTT (2 mM DTT, 1h) as indicated. To abolish targeting of the mRNA to the ER, three hydrophobic leucine residues in the signal sequence were replaced by three charged arginine residues. MKKFQLFSILSYFVALFLLPMAFA (WT) to MKKFQ**R**FS**I**RSYFVA**R**FLLPMAFA. Silent mutations were created by changing one nucleotide in each of the three leucine residues (above) without changing the amino acid.

2.2.5 Mutational Analysis of *Bip1* mRNA Cleavage Site

Bip1 mRNA mutants were generated by Marcy Diaz. Northern blot analysis was performed in collaboration with Marcy Diaz.

Mutational analysis of the cleavage site confirmed that specific sequences are required. Mutation of G373 to C or U and its deletion together with preceding nucleotides abolished Ire1-dependent *Bip1* mRNA processing (Fig. 25). By contrast, a mutation of the preceding G370 to C diminished cleavage only marginally (<2-fold). In all analyzed mutants of *Bip1* mRNA, UPR-induction increased abundance of the transcript ~2-fold (a level comparable to that observed in *Ire1Δ* cells) (Fig. 19, right panel), whether processing took place or not, perhaps due to compensatory transcriptional regulation that is independent of Ire1. For all mutants, however, the increased abundance stayed below of the 4-fold increase observed for wild type *Bip1* mRNA. To sum up, *Bip1* mRNA is truncated by an Ire1 mediated cleavage event.

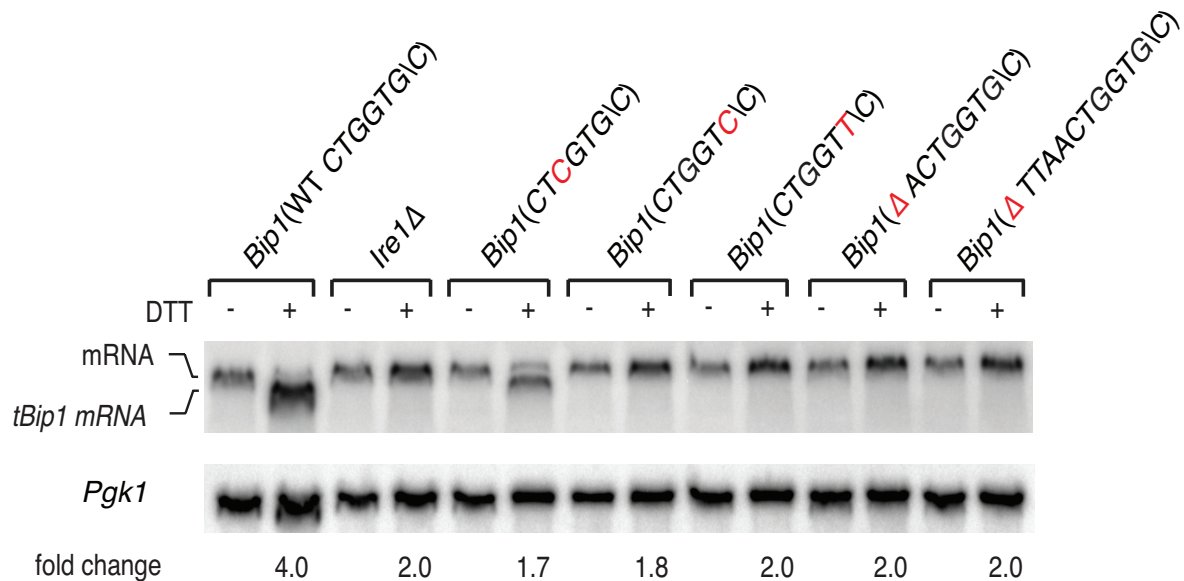


Figure 25. Mutational analysis of *Bip1* mRNA cleavage site by Northern blot.

Total RNA was extracted from wild type, *Ire1Δ* or cells carrying mutations in the *Bip1* 3' UTR mRNA. Cells were treated with 2 mM DTT, 1 h or left untreated as indicated. The fold-changes indicate *Bip1* mRNA abundance relative to that of *Pgk1* mRNA.

2.2.6 *Bip1* mRNA Processing Represents a Singularity

Deep-sequencing -rRNA library was generated in collaboration with Marcy Diaz. Data were analyzed by me.

As *Bip1* mRNA truncation resulted in a loss of the poly(A) tail, this result resolves the paradox of why *Bip1* mRNA appeared to be down-regulated in the polyA⁺ mRNA pool analyzed in Figure 5. Indeed, by directly comparing the UPR-dependent fold-change in mRNA abundance of polyA⁺ RNA and rRNA-depleted total RNA uniquely positions *Bip1* sequences as an anti-correlated outlier, whereas all other mRNAs were well correlated between the samples (Fig. 26). From these data it can be concluded that, remarkably, *Bip1* mRNA is the only stable mRNA in the cell that loses its poly(A) tail upon UPR induction.

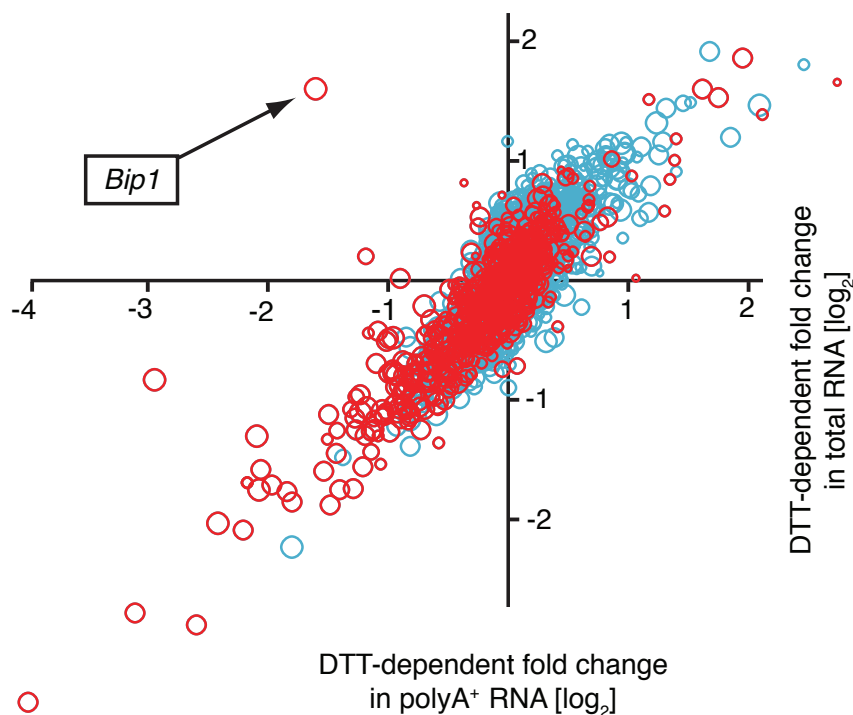


Figure 26. Genome-wide DTT-dependent gene expression from rRNA-depleted cells.

Strand-specific, mRNA enriched (after removal of ribosomal RNA) deep-sequence analysis of annotated ORFs (y-axis) compared to strand-specific polyA⁺ enriched mRNA deep-sequence analysis of annotated ORFs (x-axis) (see Fig. 1- source data). The plot indicates the ratio of transcript abundance in unstressed versus DTT-stressed (2 mM DTT, 1 h) wild type cells. Symbol sizes and colors are as described in Fig. 9.

2.2.7 Truncated *Bip1* mRNA is Efficiently Translated

Polyribosome profile was performed by Marcy Diaz. Western-blot was performed by me. It was unexpected to find a mRNA that had lost its poly(A) tail to be more stable in cells.

To determine the translation proficiency of *tBip1* mRNA, UPR-induced cells were subjected to polysome profiling. These experiments confirmed that despite lacking its poly(A) tail, *tBip1* mRNA sedimented in the polyribosome fractions in sucrose gradients (Fig. 27).

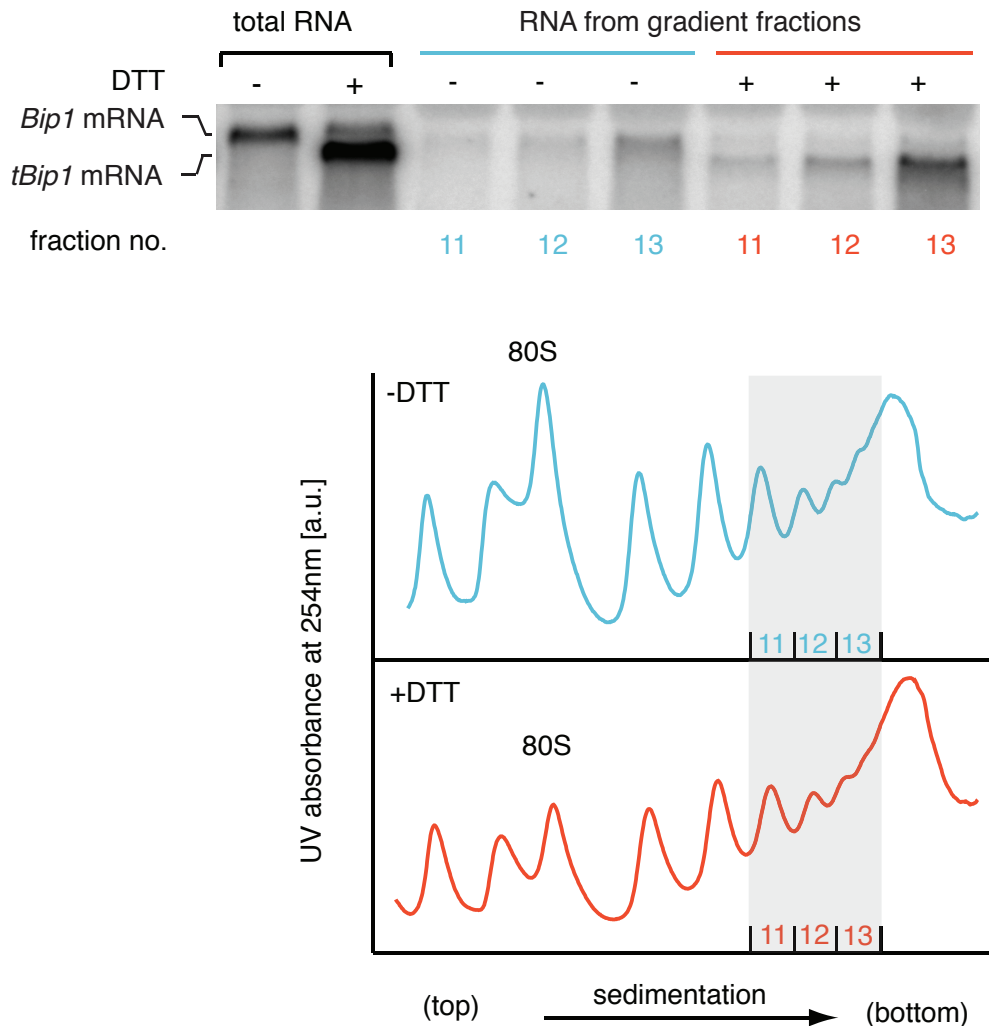


Figure 27. Polyribosome profile of *Bip1* mRNA

Northern blot analysis of the distribution of total or *tBip1* mRNA in polyribosomes from extracts of unstressed or ER-stressed (2 mM DTT, 1h) cells. Fractions 11, 12, 13 of the sucrose gradients (lower panels) were analyzed by Northern blotting (upper panels).

Moreover, ribosome footprinting demonstrated that *Bip1* mRNA in uninduced cells and *tBip1* mRNA in UPR-induced cells were engaged with actively translating ribosomes, mapping to the *Bip1* ORF (Fig. 28). The larger number of reads obtained upon UPR induction correlated with the higher abundance of *tBip1* mRNA. Thus, translation of the processed mRNA resulted

in an enhanced steady-state concentration of Bip1 protein, as shown by quantitative Western blotting (Fig 29).

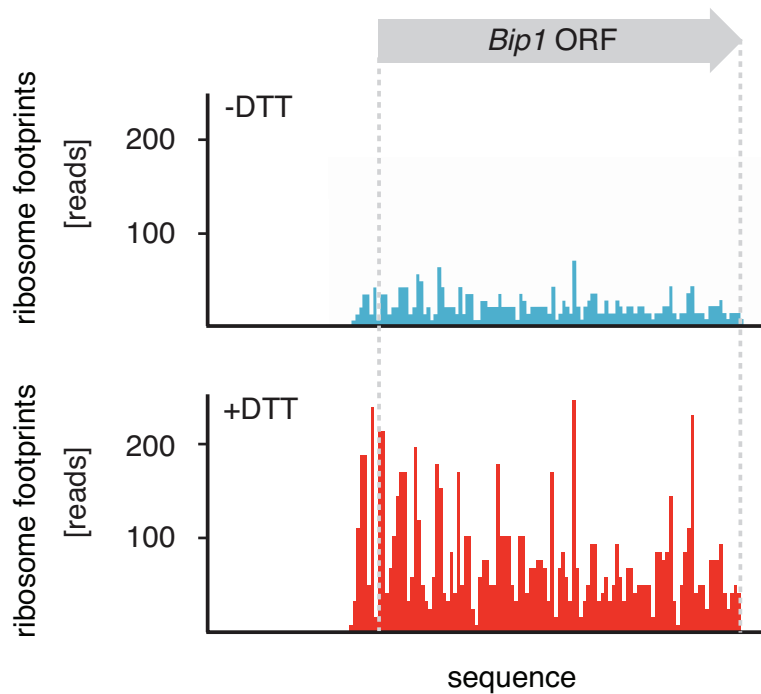


Figure 28. Ribosome footprints of *Bip1* mRNA in unstressed or ER stressed cells

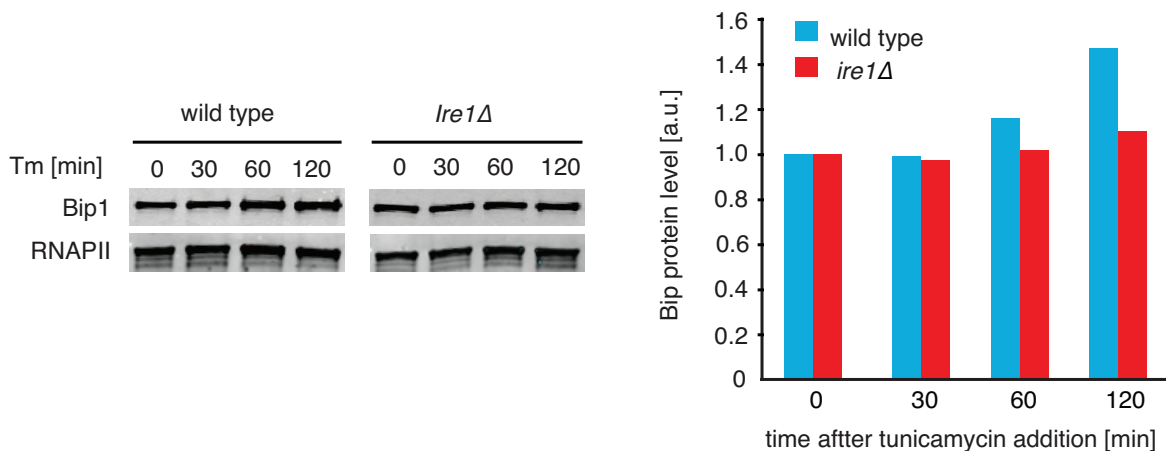


Figure 29. Western blot of Bip1 and quantitation

Left panel: Western blot of Bip1 and, as a loading control, RNA polymerase II CTD repeat (RNAPII). Wild type and *Ire1Δ* cells were treated with tunicamycin 0.5 $\mu\text{g/ml}$ and samples were taken at indicated time points. Lower panel: Quantification of Western blotting with values normalized to RNAPII.

2.2.8 *Bip1* mRNA Processing is Important for Cell Fitness

To assess the physiological consequences of this unique regulatory mechanism of Bip1 expression, the growth of strains carrying a mutation of the *Bip1* mRNA processing site

(Δ TTAACTGGTG\C) were explored. Liquid cultures of *Bip1* mRNA mutant, that were exposed to a pulse of ER stress (tunicamycin) and allowed to recover after washout of the drug showed a marked growth delay in early log phase (Fig. 30) and a decreased colony forming ability (Fig. 31), indicating that *Bip1* mRNA processing is important for maintaining cell fitness in the face of ER stress.

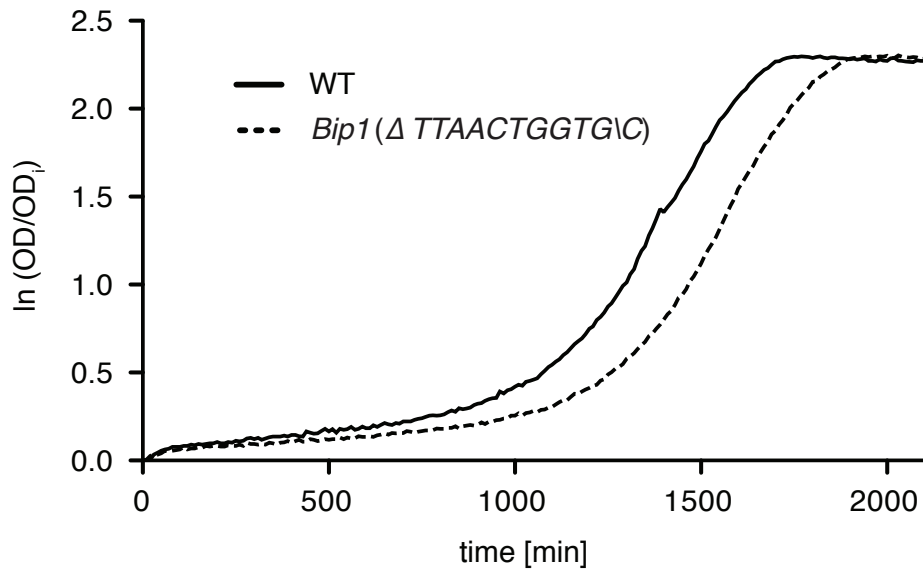


Figure 30. Growth assay of wild type and *Bip1* cleavage mutant cells after pulse of ER stress

Cell growth of wild type cells and cells carrying a deletion of *Bip1* mRNA cleavage sites (*Bip1*(Δ TTAACTGGTG\C)). Cells were treated with tunicamycin (0.5 μ g/ml) for 3 h and then recovered from ER stress by washing out the drug and re-seeding in warm fresh media. Optical density (OD) at 660 nm was measured immediately afterwards in 10 min intervals

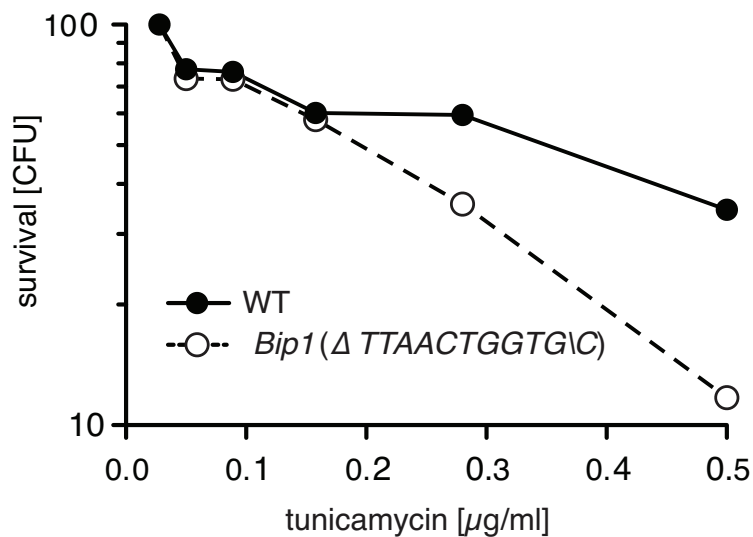


Figure 31. Colony forming unit assay of wild type and *Bip1* cleavage mutant cells upon ER stress

Growth assay setup of the same cells as in figure 30. The percentage of cells was determined by counting the number of colony-forming units (CFU) after growth for 3 h at varying tunicamycin concentrations.

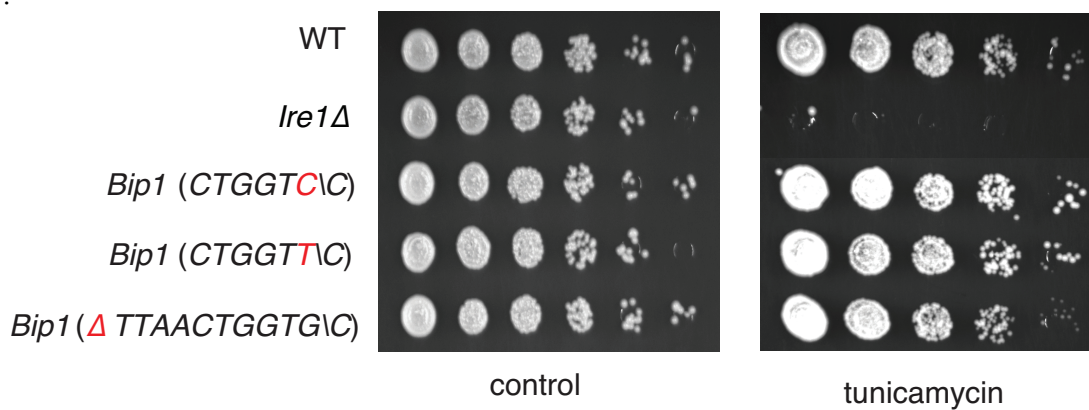


Figure 32. *Bip1* cleavage mutants on solid media inducing ER stress Spot assay by serial dilution of wild type, *Ire1* Δ and different *Bip1* mRNA cleavage mutants spotted on solid media with or without 0.03 $\mu\text{g/ml}$ of the ER stress inducer tunicamycin. Plates were photographed after 3 days of growth at 30°C.

In contrast to cell growth in liquid culture, *Bip1* mutant cells grew on UPR-inducing tunicamycin plates only marginally worse than wild type cells (Fig. 32). The importance of *Bip1* mRNA processing, therefore, varies with growth conditions.

3. Discussion

The Unfolded Protein Response in Fission Yeast

We have begun to characterize the UPR in fission yeast. To our surprise, we discovered that—by contrast to all other eukaryotes studied to date—*S. pombe* does not utilize Ire1, the most ancient ER stress sensor, to control transcription. Rather, *S. pombe* exclusively relies on two means of Ire1-dependent *post*-transcriptional regulation to cope with ER stress:

- i) Regulated Ire1-dependent mRNA decay (RIDD) of a large and highly select set of mRNAs, all of which are predicted to be translated by membrane-bound ribosomes at the ER. The mechanistic features of mRNA degradation in *S. pombe* are highly reminiscent of RIDD previously described in insect and mammalian cells, where it accompanies Ire1-dependent mRNA splicing.
- ii) Processing of *Bip1* mRNA within its 3' UTR, leading to loss of its poly(A) tail, which—counter-intuitively—results in its stabilization. The mechanistic features of this unprecedented mRNA processing step resemble the initial Ire1-dependent nucleolytic step of RIDD but *Bip1* mRNA then escapes further decay.

Our results shine new light on how ER homeostasis can be maintained and underscore the fascinating divergence of solutions that different species evolved to achieve this task.

The Physiological Role of RIDD in *S. pombe*

ER stress arises from insufficiencies in handling the protein-folding load in the ER lumen. Homeostasis, therefore, can be reestablished in two principal ways: increasing the capacity of the ER to handle the load—or decreasing the load to meet the capacity. Here we show that mRNA decay can serve as the sole means of resolving ER stress without transcriptional up-regulation of classical UPR target genes. The identified transcripts targeted for RIDD compose a subset of mRNAs, all encoding proteins that reside in or traverse the secretory

pathway. Being translated by membrane-bound ribosomes, these mRNAs are therefore in an appropriate cellular location to meet activated Ire1.

As all proteins encoded by RIDD target mRNAs enter the ER lumen, their synthesis by definition contributes to the burden of the ER protein folding machinery. RIDD therefore helps reduce the protein-folding load. It is less clear however whether such reduction would have a major impact. Indeed, a back-of-the-envelope calculation indicates that in *S. pombe* RIDD reduces the total protein influx into the ER by only 15%, even under the severe ER stress conditions explored here experimentally. This estimate derives from our ribosome footprinting data in normal versus ER-stressed cells: We scored the relative translational engagement of all mRNAs encoding proteins displaying signal sequences or transmembrane regions to estimate flux of newly synthesized polypeptides in to the ER and calculated the impact of RIDD on this set (see Material and Methods). It is difficult to envision how a mere 15% reduction of bulk protein flux into the ER would suffice to alleviate an otherwise lethal ER stress.

It is possible that RIDD preferentially targets proteins that are particularly difficult to fold and hence might have a disproportional impact on the protein folding load in the ER lumen. Indeed, Ire1 may be localized to the vicinity of mRNAs encoding such proteins by interactions of its ER luminal unfolded protein sensing domain with portions of the nascent polypeptide chains that have entered the ER lumen, as previously proposed[59,77]. An alternative and not mutually exclusive view poses that RIDD qualitatively changes the gene expression profile. In support of this notion, we notice that the population of RIDD target mRNAs is highly selective. mRNAs encoding proteins involved in lipid metabolism are highly enriched (31% of RIDD target mRNA as compared to 6.7 % in all ER-targeted mRNAs). Moreover, we find that RIDD targets encoding proteins involved in sterol metabolism are particularly enriched (13% as compared to 1.3 %). How reduced sterol synthesis would counteract the toxic effects of ER stress remains unclear. One possible explanation would be that ER stress limits sterol exit through vesicular transport and a compensatory reduction in sterol synthesis becomes important to sustain basic ER functions, perhaps by maintaining appropriate membrane fluidity [73,74,78]. In this way, RIDD (akin to other degradative pathways) could adjust basic metabolic parameters in the cell [79].

RNA Cleavage and Recognition

Previous work strongly suggests that Ire1 is the nuclease that initiates RIDD in metazoan cells [60,64,68]. Our results provide two further lines of evidence in support of this view: first, we show that and Ire1 RNase active site mutant, *Ire1(H1018N)*, is unable to sustain cell growth on ER stress-inducing media. This mutation was designed to block catalysis while retaining hydrogen-bonding interactions of the amino acid side chain. Indeed, the equivalent single amino acid substitution in *S. cerevisiae* Ire1, Ire1(H1080N), reduces catalytic activity by $>10^5$ -fold. Otherwise, Ire1(H1080N) is indistinguishable from wild type Ire1, both in its oligomerization and structural properties as determined by crystallography [80]. Second, we showed that cleaved RIDD target mRNAs carry a 2',3'-cyclic phosphate group, which is a prerequisite for the ligation reaction (tRNA ligase) used in the genome-wide mapping of mRNA ends created upon ER stress. Ire1 and tRNA endonuclease (and the Ire1-family member RNase L found in mammalian cells) are the only cytoplasmic nucleases known to produce such products.

In *S. cerevisiae*, Ire1 has a single known substrate, *Hac1* mRNA. *Hac1* and *XBPI* mRNA have highly conserved and readily recognizable stem loop structures that demarcate the splice sites [61]. Cleavage occurs at a universally conserved G always found at position 3 in the seven-base loop [47]. This information is interchangeable between species: constructs derived from *S. cerevisiae* *Hac1* mRNA are properly spliced in mammalian cells, and yeast Ire1 recognizes and precisely cleaves *XBPI* mRNA-derived substrates. We show that RIDD target mRNAs contain a short three-base UGC consensus at the Ire1 cleavage site where cleavage occurs after the G, consistent with cleavage specificity previously assigned to Ire1[47].

Thus by contrast to our understanding of the RNA-elements directing Ire1-cleavage that initiates *Hac1* and *XBPI* mRNA splicing, the information that directs mRNAs into RIDD remains vastly underspecified. By chance, UGC triplets occur much more frequently (1 to 64) in mRNAs than Ire1 cleavage sites. Therefore, the information that specifies an mRNA as an Ire1 substrate must require additional elements. Potential determinants may lie in sequence or secondary structure determinants that to date have escaped bioinformatics identification. We and others note that many of the identified cleavage sites lie in loops of potential hairpin structures [66,81]; however, the position of the scissile G in the loops is not conserved. These

structures therefore do not provide a structurally plausible explanation. Alternatively, Ire1's luminal domain may become preferentially engaged with nascent polypeptide chains that display higher affinity and/or longer exposed peptide sequences, thereby selecting mRNAs co-translationally by recognizing features in the encoded protein. The concept of Ire1 recruitment, whether through interactions via the nascent chain or elements in the mRNA *per se*, is supported by our finding that mutation of one cleavage site (UG\C -> UC\U) in *Gas2* mRNA gives rise to cleavage at alternative sites. These data indicate that local proximity rather than the RNA sequence surrounding the immediate cleavage site may guide substrate selection.

In order to stabilize the primary Ire1 cleavage products, we used mutant cells impaired in exosome function catalyzing 3' -> 5' RNA degradation. [82,83] Intriguingly, we observed that *Gas2* mRNA decay in *Ski2Δ* mutant strains was observed only transiently, peaking at 30 min after ER stress induction. This kinetic behavior suggests that clearance of Ire1-cleavage products by Ski2 may be a requirement for continued Ire1 activity. Thus, initiation of RIDD by Ire1 and further decay by the cytosolic mRNA degradation machinery may be obligatorily coupled.

Processing of *Bip1* mRNA

The observation that *S. pombe Bip1* mRNA changes size upon ER stress dates back to 1992 [76]. To date, *Bip1* mRNA processing has not been observed in any other species. The phenotypic observation of the mRNA size shift has been deployed many times as an ER stress indicator, but, surprisingly, its origin has not been investigated [84]. As we suggest here, *Bip1* mRNA is also cleaved by Ire1, yet escapes decay. The Ire1 cleavage site shares the same features described above for RIDD target mRNAs. During ER stress -induced processing, *Bip1* mRNA loses a portion of its 3' UTR and poly(A) tail. The resulting processed *tBip1* mRNA is more stable and hence is present at an increased steady-state concentration. A plausible explanation for the increased stability of *tBip1* mRNA is the loss of an RNA degron located in the severed portion of the 3' UTR. *tBip1* mRNA is actively translated with its ribosome density paralleling its increased abundance. Although poly(A) tails are generally linked to stability and translational efficiency, histone mRNAs, which likewise lack poly(A) tails, provide precedence for such an exception to the rule [85]. Histone mRNAs terminate in

a well-conserved 3' stem-loop structure, which protects from exonucleolytic degradation. Proteins binding there functions akin to the poly(A) binding proteins found on other mRNAs to enhance histone mRNA translation by looping back to the 5' cap structure [86].

Why *tBip1* mRNA escapes decay remains to be explored. Possible explanations include the presence of secondary structure elements. Indeed, we find a predicted conserved hairpin structure at the 3' termini of *tBip1* RNAs in some fission yeasts (*S. pombe*, *S. octosporus* and *S. cryophilus*); however preliminary mutational analysis failed to validate its importance for mRNA stability in *S. pombe*. An alternative possibility is that the 3' end of *tBip1* mRNA may be covalently modified. Such modification would need to be restricted to the 2'-OH, because the 3'-OH group is still accessible for modification by RNA ligase (Fig 3d). In this regard, *tBip1* mRNA would resemble miRNAs, which are 2'-O-methylated, conferring resistance to degradation [87].

Our data show that *Bip1* mRNA is the only mRNA in *S. pombe* in the expressed genome that is subject to this unique regulation. Why would such a singular mechanism have evolved exclusively for Bip1? From work in other species, Bip1 emerges as the most pleiotropically important and precisely controlled ER chaperone [88]. Moreover, Bip1 holds a unique position in *S. pombe*, where it is glycosylated [89]. A recent comprehensive gene interaction map revealed that Ire1 in *S. pombe* clusters tightly with enzymes involved in the quality control cycle of glycosylated proteins (UDP-glucose-glycoprotein glucosyltransferase, pointing toward a unique connection between glycosylation and ER stress. By contrast, corresponding E-maps in *S. cerevisiae* succinctly confirm the long-appreciated linear relationship between Ire1 and Hac1 [90]. One may speculate that ER stress in *S. pombe*, as in other species, enhances turnover of glycosylated proteins and that the regulation of *Bip1* mRNA is beneficial to its stability by compensating for such loss [79].

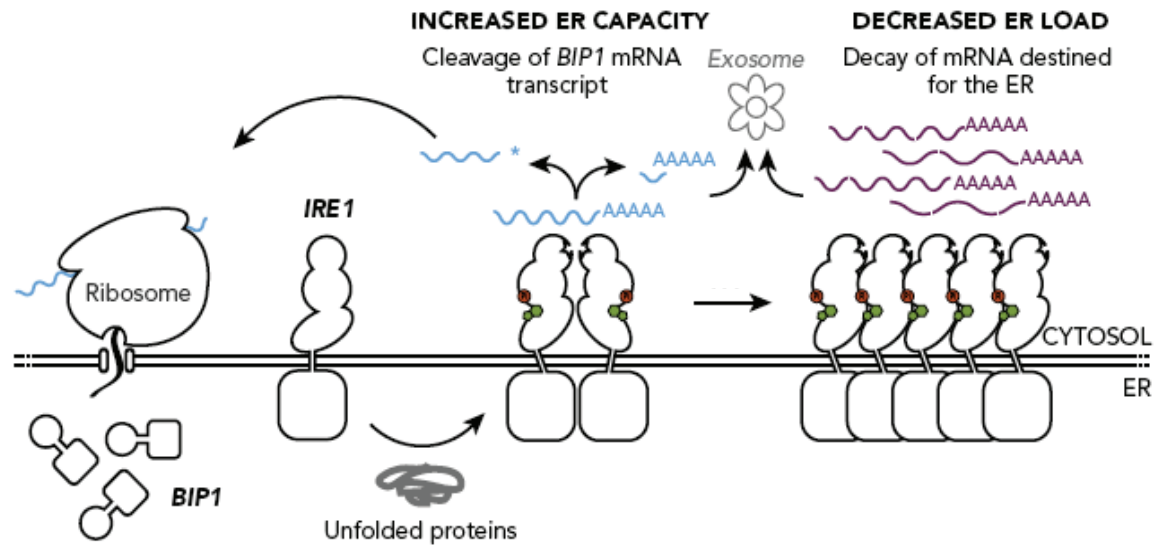


Figure 33. Model of the Unfolded Protein Response in fission yeast

Degradation of ER-targeted mRNAs by Ire1 upon ER stress. The mRNA decay reduces protein load into the ER (known as RIDD in metazoans). Additionally, Ire1 cleaves *Bip1* mRNA in its 3' UTR, stabilizing it and thereby increasing translation of Bip1 chaperone (adapted from Cross and Ron, 2012).

Conclusion

From an evolutionary angle, the UPR in *S. pombe* provides an intriguing example of how molecular machines can be repurposed. While input (unfolded proteins, ER stress) and output (RNA cleavage) have been conserved, both detail and global consequences of downstream processes have been adapted to serve different needs. The UPR in both *S. cerevisiae* and *S. pombe* fulfills a cytoprotective role, yet the mechanisms of executing this task are opposed. In *S. cerevisiae*, folding capacity is increased via transcriptional up-regulation; in *S. pombe* the folding load is decreased and the ER is restructured. In metazoan cells, both modes of Ire1 activity are merged, and depending on condition and cell type can serve different purposes. RIDD can protect cells by removing major secretory protein loads, as it is the case in insulin secreting cells [65], or it can serve to activate apoptotic pathways, as it is the case in cells experiencing prolonged and unmitigated ER stress [68].

It has always been puzzling how a strictly cognate system, such as the Ire1- and Hac1-mediated UPR regulatory pathway, would have evolved. While we cannot ascertain what represents the ancestral state, it is tempting to speculate that a broader mRNA degradation pathway preceded the development of the more specialized splicing mechanism. The prevalence of a much broader scope of Ire1 targets in *S. pombe* suggests that a primitive UPR may have served primarily as an ER-localized yet promiscuous RNA degradation system. Individual mRNA substrates would then have evolved appropriate affinities for the enzyme, rendering them more or less susceptible substrates. In this way, the stem/loop splice sites of *HAC1/XBP1* mRNAs could be the result of a long time optimization process: duplication of the cleavage site with concomitant recruitment and repurposing of tRNA ligase would have culminated the UPR splicing reaction. In this view, *S. cerevisiae* emerges as the endpoint of an optimization process rather than an evolutionary precursor. By losing the more ancient RIDD function of the UPR, *S. cerevisiae* cell would have developed to rely exclusively on a more refined and more powerful transcriptional regulation program (see also figure).

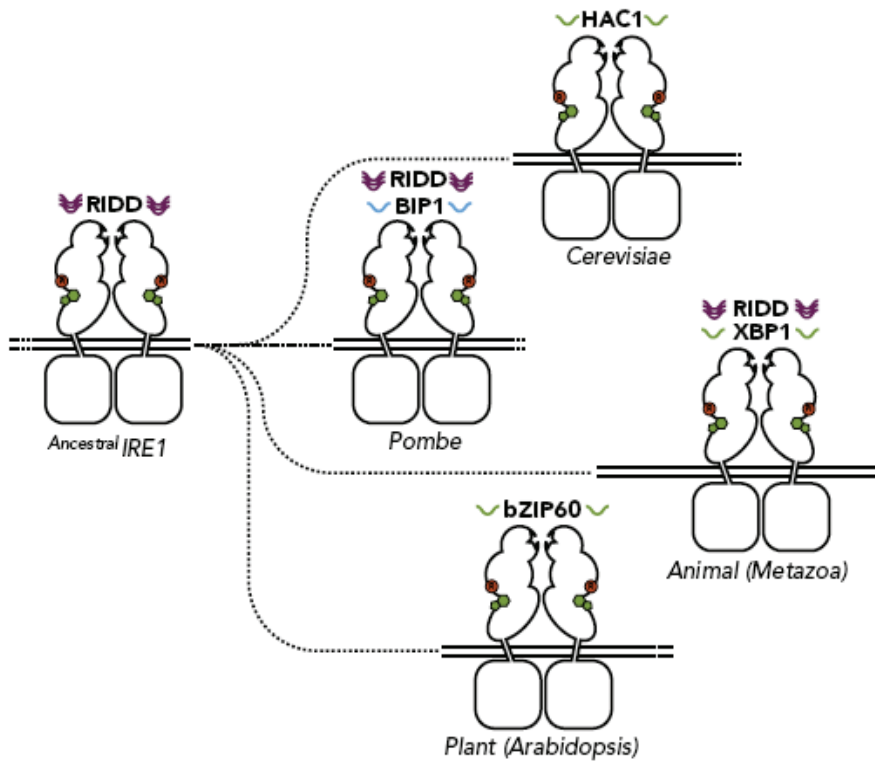


Figure 34. The UPR in different species

Ancestral Ire1 potentially have possessed mRNA decay activity (RIDD). *S. cerevisiae* (top), animals (middle) and plants (bottom). In all three branches - *S. cerevisiae* (top), animals (middle) and plants (bottom), Ire1 mediates mRNA splicing to regulate the expression of various transcription factors (Hac1, XBP1 and bZIP60). Metazoan Ire1 degrades mRNAs (RIDD), a phenomenon, which is not evident in *S. cerevisiae* and plants. Fission yeast UPR is different. It uses RIDD and a direct post-transcriptional stabilization of the molecular chaperone Bip1 (adapted from Cross and Ron, 2012).

4. Materials and Methods

4.1 Nomenclature

The unified convention used in this thesis for genes and proteins is based on the treatment by Alberts, et al. in *Molecular Biology of the Cell* (5th edition, Garland Publishing), page xxxii. In brief, all genes are denoted in italics with a capitalized first letter. Mutant alleles are indicated by appending a descriptor to the gene name. Proteins are indicated in Roman letters.

4.2 Molecular Biology methods

Standard methods and protocols were derived from “Current Protocols in Molecular Biology” (Sambrook and Russel, 2001). All chemicals used for the experiments were obtained from Sigma-Aldrich, Invitrogen, VWR and except when stated otherwise. Oligonucleotides were obtained from IDT DNA technology.

Polymerase chain reaction

The polymerase chain reaction (PCR) was used to amplify double stranded DNA fragments. Primers were designed with an average melting temperature of 55°C including a GC-clamp on the 3' end. Cycling and annealing temperature conditions were chosen depending on the fragment length and primer composition. For cloning purposes Phusion® High-Fidelity DNA Polymerase (Fermentas) was used, otherwise Taq DNA Polymerase (Fermentas).

PCR purification

DNA fragments were purified with QIAquick PCR purification Kit (Qiagen) according to the manufacturer's protocol.

Agarose gel electrophoresis

DNA fragments were separated and detected by a standard agarose gel electrophoresis using ethidium bromid DNA staining or SYBR® Safe DNA Gel Stain (Invitrogen). Briefly, agarose (Invitrogen) dissolved in TAE buffer (40mM Tris / acetic acid, pH7.5; 1mM EDTA) was

heated up in a microwave oven, and poured into a casting chamber. For optimal separation of DNA fragments, agarose concentration was ranging between 0.6% and 1.5%, depending on DNA length. To estimate DNA fragment size a standard 1 kb plus ladder (Fermentas) was used. DNA samples were mixed with 10x loading dye (50mM Tris /HCl pH7.6, 0.25% (w/ v) bromophenol blue, 0.25% xylene cyanol, 60% (v / v) glycerol) and loaded on the polymerized gel. Running time of electrophoresis was around 30 min at 120V. After separation, Gel was visualized under UV light in a gel documentation system. For preparative usage, DNA fragment of interest was sliced out of the gel and gel-purified.

Enzymatic digestion

Amplified DNA fragments and plasmids were digest with appropriate restriction enzyme(s) (NEB) to linearize plasmids or to generate complementary ends for ligation. Digestions were performed according to manufacturer's recommendation at 37 ° for 2-3 h. Afterwards, restriction enzyme(s) were heat deactivated and fragments were purified.

Plasmid DNA dephosphorylation

To avoid spontaneous re-ligation of digested plasmids, DNA fragments were dephosphorylated at their 5' position by calf intestinal phosphatase (CIF from Fermentas). Since digestion buffer are compatible with CIF phosphates, simply the addition to the reaction were added according to manufacturer's protocol. After 30 min incubation at 37°C enzymes were heat deactivated and purified by gel electrophoresis or by quick clean-up reaction kit (Qiagen).

Ligation

Digested DNA fragments and plasmids were ligated with the Rapid ligation kit (Thermo scientific) according to manufacturer's protocol. Briefly, 50-100 ng of linearized, dephosphorylated plasmid DNA and 3-4 molar excess of insert DNA were incubated with T4 DNA ligase for 20 min at room temperature. Ligation product was transformed into *E.coli*.

In vitro run-off transcription

RNA *in vitro* synthesis was carried out with MAXIscript®T7 Kit from Ambion.

DNA template was amplified by PCR including a T7 promoter (22bp) and PCR product was gel purified. 1 µg of DNA template was mixed, with rNTPS, radioactive alpha-32P UTP,

transcription buffer and RNA polymerase and incubated for 30 min at 37°C. To degraded DNA 1µl of Turbo DNase was added and incubated for additional 15 min at 37°C. The reaction was stopped by addition of 1 µL of EDTA (0.5M). For protection assay it was necessary to further purify the full-length probe by gel purification.

RNA purification

Total RNA was purified by standard hot-phenol extraction [91]. Briefly, cells (around 5-10 OD) were harvest by centrifugation or filtering, pellet was shock frozen in liquid- nitrogen and stored at -80°C. Samples were thawed, washed with DEPC water and resuspended in TE buffer (DEPC H₂O, 1 mM sodium-actetat, 5 mM EDTA). After adding SDS (f.c) and acid saturated phenol (pH 5.2), cells were broken by rigorous vortexing for 10 min at 65°C. After 5 min incubation on ice, samples were centrifuged at 15,000 rpm for 5 min. Supernatant containing RNA was transferred to a phase lock tube with 250 µl of chloroform. Phases were separated by centrifugation (15,000) for 5 min and water-phase was transferred to RNase free Eppendorf tubes. RNA was precipitated by adding sodium-acetate, 2.5 vol. (v/v) of ethanol and stored for 1 h at -80°C. RNA was pelleted by centrifugation (max. speed) for 30 min at 4°C and washed once with 75% ethanol and once with 100% ethanol. After air-drying, RNA were re-suspended in DEPC-treated water and quantified by spectrophotometry.

Northern blotting electrophoresis

Electrophoresis, Northern blotting, labeling, analysis and quantification were performed as described [48]. 10-20 µg of total RNA were loaded on 6.7 % formaldehyde and 1-1.5 % agarose gels and run in 1 × E buffer (20 mM MOPS [pH 7.0], 5 mM NaOAc, 0.5 mM EDTA) between 4-6 hours. The RNA was transferred to Duralon-UV membrane (GE Healthcare) for 18-24 hours. After cross-linking with 1500 mJ (BioRad cross-linker), the membrane was probed overnight at 65°C in Church hybridization buffer (0.5 M NaPO₄ (pH 7.2), 7% SDS, 1 mM EDTA). The membranes were subsequently washed in 0.5–1 × SSC + 0.5% SDS and exposed. Quantitation of Northern blots was performed on a Molecular Imager System.

Denaturing urea polyacrylamide gel electrophoresis (urea PAGE)

RNA was separated and detected by using a standard denaturing urea polyacrylamid gel electrophoresis. First, gel plates were cleaned and assembled. To gain optimal resolution of

the RNA, acrylamid (40% stock solution) percentage varied between 5-10 %. For a medium size gel (25 cm x 50 cm) 50 ml gel solution was prepared: 1x of TBE (stock solution: 10x TBE buffer: 1 M Tris, 0.9 M boric acid, and 0.01 M EDTA), 5-10 % acrylamid (f.c.), 8 M urea and RNase free water. To activate gel polymerization 250 µl of 10% APS and 50 µL of TEMED was added, quickly mixed and carefully poured (avoiding bubbles). After 3-4 hours of polymerization gel was pre-run to obtain optimal conditions. RNA samples were mixed with RNA gel loading buffer II (Ambion: 4x), denatured for 3 min at 95°C. After storing on ice for 5 min, samples were loaded and run at 2,000 volt (constant) for 4-5 hours. After successful separation, gel was carefully dissembled transferred on two layers of whatman paper, covered with plastic wrap and vacuum-dried for 2 hours at 65°C. Gel was exposed to a PhosphorImager.

Ribonuclease Protection Assay

In general, a Ribonuclease Protection Assay (RPA) is sensitive procedure to detect and quantify RNA species in a complex sample of total RNA. To the assay was carried out with the RPA III™ Kit (Ambion) according to the manufacturer's protocol. Samples were loaded and separated on a denaturing urea gel.

Strains, plasmids and growth conditions

Standard media and genome engineering methods for fission yeast were used as described previously [92]. Strains and plasmids used in this study are listed in Table S1. Deletion strains were generated by PCR-based homologous recombination strategies. Mutant alleles were integrated by the pop-in/pop-out method using the integrative plasmid pJK210 (*ura4*) [93]. reporter constructs were integrated into the *Leu1* locus using plasmid pJK148. All experiments were carried out in yeast extract complex media (YE5S) or in Edingburgh minimal media (EMM), supplemented with 0.225 mg/ml of L-histidine, L-leucine, L-lysine, adenine and uracil at 30°C, unless otherwise described. For pop-in/pop-out experiments, 5-FOA media containing 1 g/l 5-fluoro-orotic acid was used.

***Bip1* mRNA linker-ligation and 3' rapid amplification of cDNA ends (RACE)**

Total RNA (10 µg) from treated or untreated (2 mM DTT, 1 h) WT cells were incubated with 25 units of polynucleotide kinase (PNK) to remove 2',3'-cyclic phosphates for 1 h at 37°C. After deactivating the enzyme (75°C for 10 min), dephosphorylated RNA was precipitated

and re-suspended in 6 µl DEPC-treated water. After denaturing the RNA at 80°C for 5 min, a linker-ligation reaction was performed in the presence of dephosphorylated, denatured RNA, T4RNA Ligase II (NEB), RNase inhibitor (40 Units), DMSO, 50% PEG and 1 µg of 5' pre-adenylated linker (5'AppCTGTAGGCACCATCAAT/3ddC3', as described [94]. Reverse transcription was performed using a reverse complement DNA-oligonucleotide to the linker sequence. The 3' RACE reaction was performed as described [95]. Nested *Bip1*-PCR products were purified from ethidium-agarose gels and sequenced.

qPCR analysis of *Gas2* mRNA reporter

Total RNA (1 µg) was reverse-transcribed with random hexamers. 1% of the resulting cDNAs was employed for real-time PCR reactions utilizing SYBR green. The reactions were run and analyzed in a DNA Engine OPTICON 2 using the BioRad Opticon Monitor 3.0 software.

***Bip1* mRNA half-life measurement**

To determine the half-life of *Bip1* mRNA, we constructed an integrative plasmid (pJK148) containing the open reading frame and 3' UTR of *Bip1* mRNA under the control of a thiamine-regulated *Nmt1* promoter. The construct included the *Nmt1* 5' UTR. Cells were grown in EMM complete media (without any thiamine) for 24 h. Cells were then diluted into fresh EMM complete media and re-grown to an OD of 0.3. After inducing ER stress with tunicamycin (0.25 µg/ml) for 1 h, thiamine was added to 15 µM to block transcription of the *Nmt1* promoter [96]. Samples were processed at indicated time points and subjected to Northern blot analysis. A DNA probe complementary to the 5'UTR of *nmt1* was used for detection.

4.3 Microbiological methods

Preparation of competent *E. coli* cells

Before being transformed, *E. coli* cells have to be competent for exogenic DNA.

Cells were taken from an overnight culture, diluted in fresh 5 mL LB media, incubated for 2 h at 37°C, 2 mL of pre-culture were transferred to 40 mL of pre-warmed LB media. Cells were grown to an OD 0.5, incubated on ice for 15 min and centrifuged 2,500 rpm at 4°C for 15 min. Pellet was resuspended in 2 mL of Tfb1 buffer (MES 10 mM; RbCl₂, 100 mM; CaCl₂, 10 mM; MnCl₂, 50 mM; pH 5.8, with CH₃COOH), after Tfb1 volume being brought to 16 ml,

cells were incubated 15min on ice and centrifuged again at 2,500 rpm, 4°C during 15 min. Pellet was resuspended in 1.6 mL of Tfb2 (MOPS, 10 mM; RbCl₂, 10 mM; CaCl₂, 75 mM; glycerol, 15% (v / v); pH6.5 with KOH) and incubated for additional 15 min on ice. The suspension was aliquoted in sterile Eppendorf tubes and stored at - 80°C.

***E.coli* transformation**

80-100 µl of chemical competent *E.coli* cells (DHA α) were mixed with 50-100 ng purified plasmid DNA and incubated on ice for 30 min. After a heat shock at 42°C for 90 sec, the cells were kept on ice for additional 5 min. Then 500-800 µl LB was added and the cells were recovered at 37 °C for 45 min in a shaking incubator at 900 rpm. 50 - 200 µl transformed cells were plated on LB plates containing the appropriate antibiotics for overnight growth at 37°C.

Schizosaccharomyces pombe transformation

For transformation of fission yeast cells, a lithium acetate/single-stranded carrier DNA/polyethylene glycol method was used (see appendix: Paul Nurse lab manual, 2010). An overnight pre-culture was re-diluted to 0.2 OD in 50 mL fresh media (YE5S) and grown to an OD of 0.7 – 1.0 (at least two doubling times are required for optimal growth). Cells were pre-washed two times with MQ-H₂O and washed once with a LiOAC /TE solution (0.1 M LiOAc, pH 7.5; 10 mM Tris-HCl, pH 8.0, 1 mM EDTA, pH 8). Cell pellets were resuspended with a LiOAC /TE solution and 100 µL (~1.5 OD of cells) aliquoted into a 1.5 mL Eppendorf tube. 10-20 µL of homolog DNA was added: for PCR products: 0.5 µg PCR product with 500 bp homology or 10 µg PCR products with 100 bp homology; for integrative plasmids (pJK148 or pJK210): 0.5 - 1 µg of linearized plasmid were added. In addition, 10 µL of carrier DNA (denatured 10 mg/mL Salmon Sperm) was added, the mixture resuspended and incubated at room temperature for 15 min. After adding 500 µL of PEG solution (40 % (v/w) PEG_{MW 8000}; 0.1 M LiOAc, pH 7.5; 10 mM Tris-HCl, pH 8; 1 mM EDTA, pH 8) and vortexing, cells were incubated at 30°C for 50 min. Before heat shocking the cells for 10 min at 42°C, 50 µL of DMSO was added. Cells were centrifuged at 2,000 rpm for 3 min, resuspended in MQ-H₂O and plated on appropriated marker plates. For cells carrying an antibiotic marker, cells were plated after re-suspension in MQ-H₂O first onto non-selection plates for 2 days and then replica plated onto selection plates. Plates were incubated for 3-4 days at 30°C until transformants appear.

Growth assay and colony forming unit assay for *Bip1* 3'UTR mutant

WT and *Bip1*(*ΔTTAACTGGTGC*) mutant cells were grown overnight in (YE5S) media. The next morning cultures were diluted and grown until they reached an OD of 0.25. ER-stress was induced with tunicamycin as indicated. After 3 h, stressed cells were washed four times with pre-warmed YES5 media to remove the drug, the culture was readjusted to an OD of 0.25, and incubated in a 24 well plate (1 ml per well) over 32 h at 32°C. The OD was measured every 10 min in a microplate reader (Synergy 4 BioTeK). The colony forming unit assay was performed by plating washed cells at different dilutions on solid media (YE5S) and incubated for 3 days at 30°C. Colonies were counted from the dilutions series. Untreated cells served as a control.

4.4 Genome-wide methods

RNA-deep-sequencing sets:

- oligo-dT-enriched mRNA setI (including: WT, WT +DTT (2 mM, 1h) and *Ire1Δ*+DTT (2 mM, 1h))
- oligo-dT-enriched mRNA setII (including: WT, WT +DTT (2 mM, 1h) and (2 mM, 1h))
- total (-depleted rRNA) RNA set I (including: WT, WT +DTT (2 mM, 1h))
- total (-depleted rRNA) RNA set II(including: WT, WT +DTT (2 mM, 1h) and *Ire1Δ*+DTT (2 mM, 1h))
- 2',3'-cyclic phosphate 3'end mapping setI (*Ski2Δ* (2 mM DTT, 30min) *Ire1Δ Ski2Δ* (2 mM DTT, 30min))

RNA isolation for deep-sequencing library

As indicated, one of three methods was utilized to isolate RNA with specific chemical properties: polyA⁺ tail enrichment, rRNA depletion, or 3' end 2',3'-cyclic phosphate enrichment. Total RNA was prepared from cells by the hot acid phenol method [91], and subsequent enrichment performed. PolyA⁺ mRNA was purified by two sequential rounds of enrichment using oligo-dT DynaBeads (Invitrogen) according to the manufacturer's instructions. rRNA depletion was performed by first depleting all abundant RNAs smaller than 200nt using the modified protocol for isolating only large RNAs provided in the mirVana

miRNA Purification Kit (Ambion) followed by two rounds of subtractive hybridization using the Ribominus Eukaryote Kit for RNA-Seq(Invitrogen), according to the manufacturer's instructions. To sequence 2',3'-cyclic-phosphate cleavage products purified tRNA ligase (a kind gift from J.R. Hesselberth) was used to selectively ligate an RNA linker to all 2',3'-cyclic phosphates in total RNA as previously described [75]. PolyA⁺-enriched and rRNA-depleted samples were randomly fragmented under basic conditions, precipitated by standard methods, and ~50 nt fragments were size-selected by polyacrylamide gel electrophoresis as described in [97].

Ribosome footprint isolation for polysome profile and deep-sequencing library

Ribosome footprints were isolated as described in [97], with minor modifications. Briefly, 750 ml mid-log yeast cultures (+/- 30 min 2 mM DTT treatment) were harvested by filtration without the addition of cycloheximide, and were immediately flash frozen. Frozen cells were cryogenically lysed in the presence of 3 ml of frozen polysome lysis buffer (20 mM Tris pH 8.0, 140 mM KCl, 1.5 mM MgCl₂, 100 µg/ml cycloheximide, 1% Triton) on a Retsch MM301 mixer mill, and thawed lysates were subsequently clarified by centrifugation as described. ~50 A₂₆₀ units of clarified lysate was treated with 750 U of *E. coli* RNase I (Ambion) for 1 hour on ice to minimize 80S degradation. Monosomes were collected from sucrose density gradients (10-50% w/v, prepared in polysome lysis buffer: 20 mM Tris pH 8.0, 140 mM KCl, 5 mM MgCl₂, 100 µg / ml, cycloheximide, 0.5 mM DTT, 20 U / ml SUPERase-In) as described, and undigested control samples were loaded to generate polysome profiles shown in Figure 4B. RNA from monosome or polysome fractions was isolated using the hot acid phenol method. For ribosome profiling, 28-34 nt RNA fragments from the monosome fraction were size-selected by gel electrophoresis as described above.

Library preparation

Deep sequencing libraries were constructed as described in [94]. Briefly, size-selected mRNA (polyA⁺ and -rRNA) or ribosome footprints were 3'-dephosphorylated with T4 polynucleotide kinase (NEB). 3'-dephosphorylated RNA was ligated to a preadenylated miRNA cloning linker (IDT, Linker #1) using T4 RN12(tr) (NEB) rather than enzymatically polyadenylated. Subtractive hybridization of rRNA contaminants was not performed. Ligated samples were directly reverse transcribed using SuperScriptIII (Invitrogen), circularized using CircLigase (Epicenter), and PCR amplified.

General RNA-Sequencing data processing

Data from deep-sequencing analyses of total (-ribosomal RNA) RNA, polyA⁺ enriched mRNA and ribosome foot-printing were collected and the resulting sequences were aligned using the following method: the linker sequences at the 3' ends were removed prior to alignment using SOAP2.20, allowing a maximum of 2 total mismatches [98]. Ribosome footprint reads were assigned to a specific A-site nucleotide by an offset of +15 from 5' end of the read (only for ribosome foot-printing data set). All reads aligned to rRNA and tRNA were removed. To align intron-exon junction reads, all reads with no alignment against *S. pombe* genomics sequences were re-aligned against a sequence library of *S. pombe* processed protein-coding transcripts. All the alignments were performed against the most recent version of the *S. pombe* genome (the www.genedb.org/genedb/pombe/). The raw sequencing data will be available for download at NCBI GEO.

Quantification of mRNA abundance

Biological replicates (set I and set II, where available) were combined to increase read coverage. After combining sets, mRNA (ORF) transcripts with fewer than 100 reads before normalization were excluded. Next, the passed mRNAs (ORF) were normalized to reads per million total reads (rpm). Because the total number of reads may not reflect the total RNA production correctly [99], the observed count for gene g in condition k need to be normalized to the total RNA production to calculate the fold-change between two conditions. We used the following method to estimate the correct RNA abundance for given RPM values. Given conditions k and r , we calculated the expected RNA abundance of condition k given the RPM value in condition r with the following equation: $x_{k,r,g} = 2^{a_{k,r}} \log_2 x_{r,g} + b_{k,r}$

$x_{r,g}$ is the RPM value for gene g in the reference condition, $x_{k,r,g}$ is expected RPM estimated with linear regression between the RPM values from condition k and r . $a_{k,r}$ and $b_{k,r}$ are the coefficients of the linear regression where $a_{k,r} = (Y_{k,g} - Y_r) / (Y_{r,g} - Y_r)$, $b_{k,r} = Y_{k,g} - a_{k,r} Y_{r,g}$ in which $Y_{k,g} = \log_2 x_{k,g}$, $Y_{r,g} = \log_2(x_{r,g})$.

For the above linear regression, genes with $M_g = x_{k,g} / x_{r,g} \geq 10$ or ≤ 0.1 were removed from the data set to estimated $a_{k,r}$ and $b_{k,r}$. The fold change between condition k and r is then calculated as: $F_{g,k,r} = x_{k,g} / x_{r,g}$, which is the RPM value for gene g under condition k divided by the expected RPM estimated above.

2',3'-cyclic phosphate 3' end RNA mapping and Ire1 cleavage site motif determination

Sequence read alignments from the 2',3'-cyclic phosphate mapping data were performed as for the RNA-Seq reads described above. The design of the library (3' end mapping) made it necessary to align the reads to the opposed strand of the gene. To map putative Ire1-dependent cleavage sites with high stringency, we identified the positions within each transcript containing more than 4 reads in RNA derived from the *Ski2Δ* sample and zero reads in RNA derived from the *Ire1Δ Ski2Δ* sample. We identified by this method 4027 putative Ire1-dependent cleavage sites in the genome. By using a less stringent criterion (by taken the ration between *Ski2Δ* sample and *Ire1Δ Ski2Δ* sample: we allowed a ratio of 5 or more). By this criterion we identified 4134 putative Ire1-dependent cleavage sites. The overlap between the two methods is 97%. We continued our analysis with the more stringent criteria of only allowing zero reads in *Ire1Δ Ski2Δ* sample. To identify an overrepresented consensus sequence, we first extended the sequences 9 nt upstream and downstream of the potential cleavage sites. Furthermore, we used a position weight matrix (PWM), which was generated from these sequences by weighting each sequence with the reads from the *Ski2Δ* sample. By using all annotated genes and the corresponding putative cleavage sites, we could not identify overrepresented sequences. The same held true for the ER-target mRNAs set (N=1014). By contrast, a strong consensus motif (Fig. 2e) emerged when we mapped the putative cleavage sites in our set of 39 Ire1- and ER stress-dependently two-fold down-regulated transcripts.

4.5 Protein biochemistry

Protein analysis

Cells were cultured in YE5S media. Between 5 and 10 OD units were collected by centrifugation and snap-frozen. Cell pellets were thawed on ice, re-suspended in 200 μl of lysis buffer (8 M urea, 50 mM HEPES pH 7.4) and lysed in a glass bead mill (5 min at 4°C). After adding 20 μl of a 25% SDS solution, samples were incubated at 65°C for 5 min. The lysates were collected by piercing the bottom of the tubes with a syringe needle and clarified by re-centrifugation (1,000 rpm for 10 sec). Total protein concentration was determined by a standard bichromic acid (BCA) assay (manual instruction, Pierce Biotechnology). 10 μg of lysate per lane were electrophoresed on SDS-polyacrylamide gradient gels (4%-15%, BioRad). The separated proteins were subsequently transferred to PDVF membranes at 200

mA for 1 h. Blots were blocked with 5% milk in Tris-buffered saline (10 mM Tris, 150 mM NaCl, 0.1% Tween-20) and incubated with primary antibodies overnight at 4°C. Antibodies and dilutions: rabbit polyclonal anti-Kar2 (1:5000), mouse monoclonal anti-RNA polymerase II carboxy-terminal domain (CTD) repeat (Abcam ab817) (1:8000 dilution). Blots were washed and incubated with Li-Cor fluorescently-coupled secondary antibodies (1:5,000) for 30 min. Immunoreactive bands were identified using a Li-Cor infrared scanner, and processed with the Odyssey software package.

Estimation of protein flux into the ER

We scored ribosome footprint reads per kilobase (to normalize for length of open reading frames) per million reads (to compare different conditions) for the set of mRNAs, encoding proteins predicted to enter the ER as described above.

all ER-targeted mRNAs ribosome occupancies (N=1014 mRNAs)	rpkm	ration normalized to WT-DTT	[%]
WT (-DTT)	83540	1	100
WT(+DTT)	71996	0.8618147	86.18146995
ΔIRE1(+DTT)	90166	1.079315298	107.9315298

**rpkm=reads per kilo-base of transcript per million
reads**

5. Bibliography

1. Alberts BJ, A Lewis, J Raff, M Roberts, K Walter, P (2008) *Molecular Biology of the Cell*: Garland Science.
2. Bukau B, Horwich AL (1998) The Hsp70 and Hsp60 chaperone machines. *Cell* 92: 351-366.
3. Wolf DH, Hilt W (2004) The proteasome: a proteolytic nanomachine of cell regulation and waste disposal. *Biochim Biophys Acta* 1695: 19-31.
4. Powers ET, Morimoto RI, Dillin A, Kelly JW, Balch WE (2009) Biological and chemical approaches to diseases of proteostasis deficiency. *Annu Rev Biochem* 78: 959-991.
5. Lin JH, Walter P, Yen TS (2008) Endoplasmic reticulum stress in disease pathogenesis. *Annu Rev Pathol* 3: 399-425.
6. Hu J, Prinz WA, Rapoport TA (2011) Weaving the web of ER tubules. *Cell* 147: 1226-1231.
7. Shibata Y, Hu J, Kozlov MM, Rapoport TA (2009) Mechanisms shaping the membranes of cellular organelles. *Annu Rev Cell Dev Biol* 25: 329-354.
8. Shibata Y, Voeltz GK, Rapoport TA (2006) Rough sheets and smooth tubules. *Cell* 126: 435-439.
9. Rapoport TA (2007) Protein translocation across the eukaryotic endoplasmic reticulum and bacterial plasma membranes. *Nature* 450: 663-669.
10. Walter P, Blobel G (1981) Translocation of proteins across the endoplasmic reticulum. II. Signal recognition protein (SRP) mediates the selective binding to microsomal membranes of in-vitro-assembled polysomes synthesizing secretory protein. *J Cell Biol* 91: 551-556.
11. Walter P, Ibrahimi I, Blobel G (1981) Translocation of proteins across the endoplasmic reticulum. I. Signal recognition protein (SRP) binds to in-vitro-assembled polysomes synthesizing secretory protein. *J Cell Biol* 91: 545-550.
12. Walter P, Blobel G (1981) Translocation of proteins across the endoplasmic reticulum III. Signal recognition protein (SRP) causes signal sequence-dependent and site-specific arrest of chain elongation that is released by microsomal membranes. *J Cell Biol* 91: 557-561.
13. Keenan RJ, Freymann DM, Stroud RM, Walter P (2001) The signal recognition particle. *Annu Rev Biochem* 70: 755-775.
14. Bradshaw N, Neher SB, Booth DS, Walter P (2009) Signal sequences activate the catalytic switch of SRP RNA. *Science* 323: 127-130.
15. Shan SO, Chandrasekar S, Walter P (2007) Conformational changes in the GTPase modules of the signal reception particle and its receptor drive initiation of protein translocation. *J Cell Biol* 178: 611-620.
16. Lyman SK, Schekman R (1997) Binding of secretory precursor polypeptides to a translocon subcomplex is regulated by BiP. *Cell* 88: 85-96.
17. Deshaies RJ, Schekman R (1987) A yeast mutant defective at an early stage in import of secretory protein precursors into the endoplasmic reticulum. *J Cell Biol* 105: 633-645.
18. Park E, Rapoport TA (2012) Mechanisms of Sec61/SecY-mediated protein translocation across membranes. *Annu Rev Biophys* 41: 21-40.
19. Martoglio B, Dobberstein B (1998) Signal sequences: more than just greasy peptides. *Trends Cell Biol* 8: 410-415.
20. Bukau B, Weissman J, Horwich A (2006) Molecular chaperones and protein quality control. *Cell* 125: 443-451.

21. Matlack KE, Misselwitz B, Plath K, Rapoport TA (1999) BiP acts as a molecular ratchet during posttranslational transport of prepro-alpha factor across the ER membrane. *Cell* 97: 553-564.
22. Tu BP, Weissman JS (2004) Oxidative protein folding in eukaryotes: mechanisms and consequences. *J Cell Biol* 164: 341-346.
23. Parodi AJ (2000) Protein glucosylation and its role in protein folding. *Annu Rev Biochem* 69: 69-93.
24. Helenius A, Aebi M (2004) Roles of N-linked glycans in the endoplasmic reticulum. *Annu Rev Biochem* 73: 1019-1049.
25. Ellgaard L, Helenius A (2003) Quality control in the endoplasmic reticulum. *Nat Rev Mol Cell Biol* 4: 181-191.
26. Hiller MM, Finger A, Schweiger M, Wolf DH (1996) ER degradation of a misfolded luminal protein by the cytosolic ubiquitin-proteasome pathway. *Science* 273: 1725-1728.
27. Kostova Z, Wolf DH (2003) For whom the bell tolls: protein quality control of the endoplasmic reticulum and the ubiquitin-proteasome connection. *EMBO J* 22: 2309-2317.
28. Stolz A, Wolf DH (2010) Endoplasmic reticulum associated protein degradation: a chaperone assisted journey to hell. *Biochim Biophys Acta* 1803: 694-705.
29. Buschhorn BA, Kostova Z, Medicherla B, Wolf DH (2004) A genome-wide screen identifies Yos9p as essential for ER-associated degradation of glycoproteins. *FEBS Lett* 577: 422-426.
30. Walter P, Ron D (2011) The unfolded protein response: from stress pathway to homeostatic regulation. *Science* 334: 1081-1086.
31. Travers KJ, Patil CK, Wodicka L, Lockhart DJ, Weissman JS, et al. (2000) Functional and genomic analyses reveal an essential coordination between the unfolded protein response and ER-associated degradation. *Cell* 101: 249-258.
32. Friedlander R, Jarosch E, Urban J, Volkwein C, Sommer T (2000) A regulatory link between ER-associated protein degradation and the unfolded-protein response. *Nat Cell Biol* 2: 379-384.
33. Brar GA, Yassour M, Friedman N, Regev A, Ingolia NT, et al. (2012) High-resolution view of the yeast meiotic program revealed by ribosome profiling. *Science* 335: 552-557.
34. Shore GC, Papa FR, Oakes SA (2011) Signaling cell death from the endoplasmic reticulum stress response. *Curr Opin Cell Biol* 23: 143-149.
35. Tabas I, Ron D (2011) Integrating the mechanisms of apoptosis induced by endoplasmic reticulum stress. *Nat Cell Biol* 13: 184-190.
36. Hetz C (2012) The unfolded protein response: controlling cell fate decisions under ER stress and beyond. *Nat Rev Mol Cell Biol* 13: 89-102.
37. Mori K, Sant A, Kohno K, Normington K, Gething MJ, et al. (1992) A 22 bp cis-acting element is necessary and sufficient for the induction of the yeast KAR2 (BiP) gene by unfolded proteins. *EMBO J* 11: 2583-2593.
38. Mori K, Ma W, Gething MJ, Sambrook J (1993) A transmembrane protein with a cdc2+/CDC28-related kinase activity is required for signaling from the ER to the nucleus. *Cell* 74: 743-756.
39. Cox JS, Shamu CE, Walter P (1993) Transcriptional induction of genes encoding endoplasmic reticulum resident proteins requires a transmembrane protein kinase. *Cell* 73: 1197-1206.

40. Cox JS, Walter P (1996) A novel mechanism for regulating activity of a transcription factor that controls the unfolded protein response. *Cell* 87: 391-404.
41. Sidrauski C, Cox JS, Walter P (1996) tRNA ligase is required for regulated mRNA splicing in the unfolded protein response. *Cell* 87: 405-413.
42. Bernales S, Papa FR, Walter P (2006) Intracellular signaling by the unfolded protein response. *Annu Rev Cell Dev Biol* 22: 487-508.
43. Credle JJ, Finer-Moore JS, Papa FR, Stroud RM, Walter P (2005) On the mechanism of sensing unfolded protein in the endoplasmic reticulum. *Proc Natl Acad Sci U S A* 102: 18773-18784.
44. Gardner BM, Walter P (2011) Unfolded proteins are Ire1-activating ligands that directly induce the unfolded protein response. *Science* 333: 1891-1894.
45. Korennykh AV, Egea PF, Korostelev AA, Finer-Moore J, Zhang C, et al. (2009) The unfolded protein response signals through high-order assembly of Ire1. *Nature* 457: 687-693.
46. Sidrauski C, Walter P (1997) The transmembrane kinase Ire1p is a site-specific endonuclease that initiates mRNA splicing in the unfolded protein response. *Cell* 90: 1031-1039.
47. Gonzalez TN, Sidrauski C, Dorfler S, Walter P (1999) Mechanism of non-spliceosomal mRNA splicing in the unfolded protein response pathway. *EMBO J* 18: 3119-3132.
48. Ruegsegger U, Leber JH, Walter P (2001) Block of HAC1 mRNA translation by long-range base pairing is released by cytoplasmic splicing upon induction of the unfolded protein response. *Cell* 107: 103-114.
49. Calfon M, Zeng H, Urano F, Till JH, Hubbard SR, et al. (2002) IRE1 couples endoplasmic reticulum load to secretory capacity by processing the XBP-1 mRNA. *Nature* 415: 92-96.
50. Yoshida H, Matsui T, Yamamoto A, Okada T, Mori K (2001) XBP1 mRNA is induced by ATF6 and spliced by IRE1 in response to ER stress to produce a highly active transcription factor. *Cell* 107: 881-891.
51. Acosta-Alvear D, Zhou Y, Blais A, Tsikitis M, Lents NH, et al. (2007) XBP1 controls diverse cell type- and condition-specific transcriptional regulatory networks. *Mol Cell* 27: 53-66.
52. Pavitt GD, Ron D (2012) New insights into translational regulation in the endoplasmic reticulum unfolded protein response. *Cold Spring Harb Perspect Biol* 4.
53. Bertolotti A, Zhang Y, Hendershot LM, Harding HP, Ron D (2000) Dynamic interaction of BiP and ER stress transducers in the unfolded-protein response. *Nat Cell Biol* 2: 326-332.
54. Harding HP, Zhang Y, Bertolotti A, Zeng H, Ron D (2000) Perk is essential for translational regulation and cell survival during the unfolded protein response. *Mol Cell* 5: 897-904.
55. Sato N, Urano F, Yoon Leem J, Kim SH, Li M, et al. (2000) Upregulation of BiP and CHOP by the unfolded-protein response is independent of presenilin expression. *Nat Cell Biol* 2: 863-870.
56. Novoa I, Zeng H, Harding HP, Ron D (2001) Feedback inhibition of the unfolded protein response by GADD34-mediated dephosphorylation of eIF2alpha. *J Cell Biol* 153: 1011-1022.
57. Yoshida H, Okada T, Haze K, Yanagi H, Yura T, et al. (2000) ATF6 activated by proteolysis binds in the presence of NF-Y (CBF) directly to the cis-acting element responsible for the mammalian unfolded protein response. *Mol Cell Biol* 20: 6755-6767.

58. Sakai J, Nohturfft A, Goldstein JL, Brown MS (1998) Cleavage of sterol regulatory element-binding proteins (SREBPs) at site-1 requires interaction with SREBP cleavage-activating protein. Evidence from in vivo competition studies. *J Biol Chem* 273: 5785-5793.
59. Hollien J, Weissman JS (2006) Decay of endoplasmic reticulum-localized mRNAs during the unfolded protein response. *Science* 313: 104-107.
60. Hollien J, Lin JH, Li H, Stevens N, Walter P, et al. (2009) Regulated Ire1-dependent decay of messenger RNAs in mammalian cells. *J Cell Biol* 186: 323-331.
61. Niwa M, Patil CK, DeRisi J, Walter P (2005) Genome-scale approaches for discovering novel nonconventional splicing substrates of the Ire1 nuclease. *Genome Biol* 6: R3.
62. Garneau NL, Wilusz J, Wilusz CJ (2007) The highways and byways of mRNA decay. *Nat Rev Mol Cell Biol* 8: 113-126.
63. Lee AH, Heidtman K, Hotamisligil GS, Glimcher LH (2011) Dual and opposing roles of the unfolded protein response regulated by IRE1alpha and XBP1 in proinsulin processing and insulin secretion. *Proc Natl Acad Sci U S A* 108: 8885-8890.
64. Cross BC, Bond PJ, Sadowski PG, Jha BK, Zak J, et al. (2012) The molecular basis for selective inhibition of unconventional mRNA splicing by an IRE1-binding small molecule. *Proc Natl Acad Sci U S A* 109: E869-878.
65. Lipson KL, Ghosh R, Urano F (2008) The role of IRE1alpha in the degradation of insulin mRNA in pancreatic beta-cells. *PLoS One* 3: e1648.
66. Hur KY, So JS, Ruda V, Frank-Kamenetsky M, Fitzgerald K, et al. (2012) IRE1alpha activation protects mice against acetaminophen-induced hepatotoxicity. *J Exp Med* 209: 307-318.
67. Upton JP, Wang L, Han D, Wang ES, Huskey NE, et al. (2012) IRE1alpha Cleaves Select microRNAs during ER Stress to Derepress Translation of Proapoptotic Caspase-2. *Science*.
68. Han D, Lerner AG, Vande Walle L, Upton JP, Xu W, et al. (2009) IRE1alpha kinase activation modes control alternate endoribonuclease outputs to determine divergent cell fates. *Cell* 138: 562-575.
69. Hooks KB, Griffiths-Jones S (2011) Conserved RNA structures in the non-canonical Hac1/Xbp1 intron. *RNA Biol* 8: 552-556.
70. Frost A, Elgort MG, Brandman O, Ives C, Collins SR, et al. (2012) Functional repurposing revealed by comparing *S. pombe* and *S. cerevisiae* genetic interactions. *Cell* 149: 1339-1352.
71. Hughes AL, Todd BL, Espenshade PJ (2005) SREBP pathway responds to sterols and functions as an oxygen sensor in fission yeast. *Cell* 120: 831-842.
72. Raychaudhuri S, Young BP, Espenshade PJ, Loewen C, Jr. (2012) Regulation of lipid metabolism: a tale of two yeasts. *Curr Opin Cell Biol* 24: 502-508.
73. Feng B, Yao PM, Li Y, Devlin CM, Zhang D, et al. (2003) The endoplasmic reticulum is the site of cholesterol-induced cytotoxicity in macrophages. *Nat Cell Biol* 5: 781-792.
74. So JS, Hur KY, Tarrío M, Ruda V, Frank-Kamenetsky M, et al. (2012) Silencing of Lipid Metabolism Genes through IRE1alpha-Mediated mRNA Decay Lowers Plasma Lipids in Mice. *Cell Metab* 16: 487-499.
75. Schutz K, Hesselberth JR, Fields S (2010) Capture and sequence analysis of RNAs with terminal 2',3'-cyclic phosphates. *RNA* 16: 621-631.
76. Pidoux AL, Armstrong J (1992) Analysis of the BiP gene and identification of an ER retention signal in *Schizosaccharomyces pombe*. *EMBO J* 11: 1583-1591.
77. Ron D (2006) Cell biology. Stressed cells cope with protein overload. *Science* 313: 52-53.

78. Nilsson I, Ohvo-Rekila H, Slotte JP, Johnson AE, von Heijne G (2001) Inhibition of protein translocation across the endoplasmic reticulum membrane by sterols. *J Biol Chem* 276: 41748-41754.
79. Bernasconi R, Galli C, Noack J, Bianchi S, de Haan CA, et al. (2012) Role of the SEL1L:LC3-I complex as an ERAD tuning receptor in the mammalian ER. *Mol Cell* 46: 809-819.
80. Korennykh AV, Korostelev AA, Egea PF, Finer-Moore J, Stroud RM, et al. (2011) Structural and functional basis for RNA cleavage by Ire1. *BMC Biol* 9: 47.
81. Oikawa D, Tokuda M, Hosoda A, Iwawaki T (2010) Identification of a consensus element recognized and cleaved by IRE1 alpha. *Nucleic Acids Res* 38: 6265-6273.
82. Anderson JS, Parker RP (1998) The 3' to 5' degradation of yeast mRNAs is a general mechanism for mRNA turnover that requires the SKI2 DEVH box protein and 3' to 5' exonucleases of the exosome complex. *EMBO J* 17: 1497-1506.
83. Gatfield D, Izaurralde E (2004) Nonsense-mediated messenger RNA decay is initiated by endonucleolytic cleavage in *Drosophila*. *Nature* 429: 575-578.
84. D'Alessio C, Fernandez F, Trombetta ES, Parodi AJ (1999) Genetic evidence for the heterodimeric structure of glucosidase II. The effect of disrupting the subunit-encoding genes on glycoprotein folding. *J Biol Chem* 274: 25899-25905.
85. Marzluff WF, Duronio RJ (2002) Histone mRNA expression: multiple levels of cell cycle regulation and important developmental consequences. *Curr Opin Cell Biol* 14: 692-699.
86. Sanchez R, Marzluff WF (2002) The stem-loop binding protein is required for efficient translation of histone mRNA in vivo and in vitro. *Mol Cell Biol* 22: 7093-7104.
87. Yu B, Yang Z, Li J, Minakhina S, Yang M, et al. (2005) Methylation as a crucial step in plant microRNA biogenesis. *Science* 307: 932-935.
88. Gulow K, Bienert D, Haas IG (2002) BiP is feed-back regulated by control of protein translation efficiency. *J Cell Sci* 115: 2443-2452.
89. Pidoux AL, Armstrong J (1993) The BiP protein and the endoplasmic reticulum of *Schizosaccharomyces pombe*: fate of the nuclear envelope during cell division. *J Cell Sci* 105 (Pt 4): 1115-1120.
90. Schuldiner M, Collins SR, Thompson NJ, Denic V, Bhamidipati A, et al. (2005) Exploration of the function and organization of the yeast early secretory pathway through an epistatic miniarray profile. *Cell* 123: 507-519.
91. Kohrer K, Domdey H (1991) Preparation of high molecular weight RNA. *Methods Enzymol* 194: 398-405.
92. Moreno S, Klar, A., Nurse, P. (1991) Molecular genetic analysis of fission yeast *Schizosaccharomyces pombe*. *Methods Enzymology*.
93. Guthrie CaF, G. (2004) *Guide to Yeast Genetics and Molecular Biology, Part A*. Academic Press: Academic Press.
94. Ingolia NT, Lareau LF, Weissman JS (2011) Ribosome profiling of mouse embryonic stem cells reveals the complexity and dynamics of mammalian proteomes. *Cell* 147: 789-802.
95. Scotto-Lavino E, Du G, Frohman MA (2006) 3' end cDNA amplification using classic RACE. *Nat Protoc* 1: 2742-2745.
96. Maundrell K (1990) *nmt1* of fission yeast. A highly transcribed gene completely repressed by thiamine. *J Biol Chem* 265: 10857-10864.
97. Ingolia NT, Ghaemmaghami S, Newman JR, Weissman JS (2009) Genome-wide analysis in vivo of translation with nucleotide resolution using ribosome profiling. *Science* 324: 218-223.

98. Li R, Yu C, Li Y, Lam TW, Yiu SM, et al. (2009) SOAP2: an improved ultrafast tool for short read alignment. *Bioinformatics* 25: 1966-1967.
99. Robinson MD, Oshlack A (2010) A scaling normalization method for differential expression analysis of RNA-seq data. *Genome Biol* 11: R25.

6. Acknowledgment

I'm very grateful to Professor Dr. Dieter Wolf who has giving me the opportunity to accept me as a PhD candidate. Over the years, he has been a fantastic advisor and I'm thankful for many fruitful discussions.

I would like to thank Prof. Dr. Peter Walter, who welcomed me in his laboratory in San Francisco. His unique style and his creative thinking inspired and encouraged me to follow the path of science with a lot of enthusiasm. I'm especially thankful to him for giving me a lot of freedom, which allowed me to find my own scientific style.

Also I would like to thank Prof. Dr. Hao Li, who scientifically supported me over the years at UCSF. Trained as physicists, he gave me a complete new way of thinking about science.

I'm also grateful to my collaborator Marcy Diaz, without her work and input this would have been not possible.

The work in the lab would have not been so fruitful, and fun without the help and presence of many great colleagues and friends. Especially, I would like to thank Tomas Aragon, Benoit Kornmann, Jiashun Zheng and Diego Acosta-Alvear.

Thanks to Silke Nock and Teresa Donovan who are keeping the enterprise (lab) running.

Last but not least I want to thank my family for their support and their patience with me.

7. Curriculum vitae

Personal data

Name: Philipp Kimmig
Address: Fallhausstraße 27
91720 Absberg, Germany
E-mail: philippkimmig@gmail.com

Education

2008 – 2013 PhD candidate: University of Stuttgart, Germany, Professor Dieter Wolf and University of California, San Francisco, USA: Professor Peter Walter
10/2000-12/2007: Master (Diplom) in technical Biology, University of Stuttgart, Germany
06/2006 – 08/2007 Master (Diplom)-Thesis, Institute of Biochemistry, University of Stuttgart: Gid2, an active subunit of a novel ubiquitin ligase (E3) complex
07/2004 – 01/2005 Senior Thesis, Institute of Microbiology, University of Stuttgart: Expression, purification and biochemical characterisation of PHA-Depolymerase PhaZ5 in *Ralstonia eutropha*
09/2000 – 07/2003 Bachelor (Vordiplom) University of Stuttgart, Germany

Publication

Kimmig, P., Diaz*, M., Zheng, J., Williams, C., Lang, A., Aragon, T., Li, H., Walter, P. (2012); *The unfolded protein response in fission yeast modulates stability of select mRNAs to maintain protein homeostasis.* eLife; 1.0048 (*authors with equal contribution)

Fordyce, PM., Pincus, D., Kimmig, P., Nelson, CS., El-Samad, H., Walter, P., DeRisi, JL. (2012); *The basic leucine zipper transcription factor Hac1 binds DNA in two distinct modes as revealed by microfluidic analyses.* Proc Natl Acad Sci USA. 2012 Oct 10.

Pfaffmann* T, Santt* O, Braun B, Kimmig P, Juretschke J, Alberts S, Regelman J, Scheel H, Hofmann K, Thumm M, Wolf DH.; *The yeast Gid-complex, homologous to the human CTLH, is a novel E3 regulating carbohydrate metabolism.* Mol Biol. Cell, 2008; 19: 3323 – 3333. (*authors with equal contribution).

Handrick R, Reinhardt S, Kimmig P, Jendrossek D. *The "intracellular" poly(3-hydroxybutyrate) (PHB) depolymerase of Rhodospirillum rubrum is a periplasm-located protein with specificity for native PHB and with structural similarity to extracellular PHB depolymerases.* Journal of Bacteriology. 2004 Nov;186(21):7243-53.